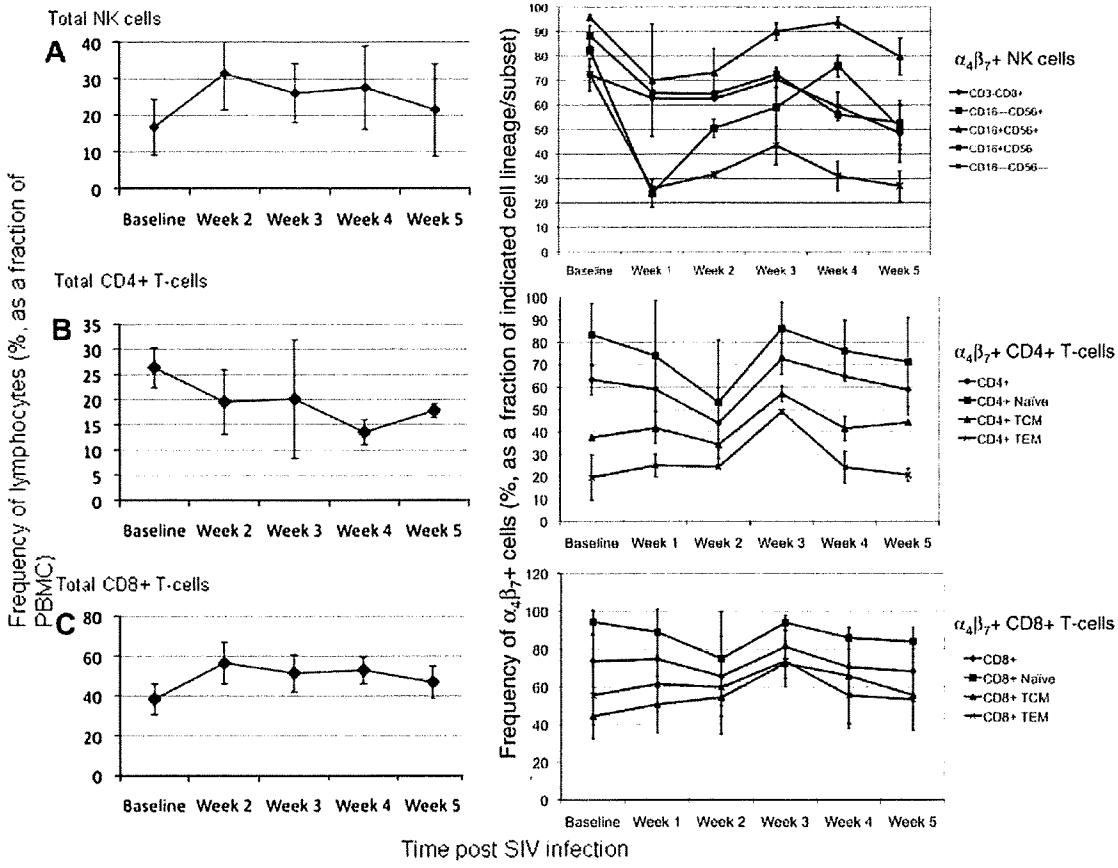

Fig. 8. Acute SIV infection in RM leads to a decline and/or mobilization of select $\alpha_4\beta_7$+ lymphocytes. Longitudinal analysis of the frequency of (A) total and $\alpha_4\beta_7$+ NK cell subsets, (B) total and $\alpha_4\beta_7$+ CD4+ T-cell subsets and (C) total and $\alpha_4\beta_7$+ CD8+ T-cell subsets during the acute phase of SIV infection in RM. The frequency of total NK cells, CD4+ T-cells and CD8+ T-cells (left panels) was determined in 4 RM that were experimentally infected with SIVmac239. Isolated PBMC were also stained with biotinylated murine $\alpha_4\beta_7$ mAb followed by streptavidin PE-Cy7 and the frequencies of indicated $\alpha_4\beta_7$+ lymphocyte subsets (right panels) in the periphery were monitored by flow cytometry every week for 5 weeks post infection. Shown are the mean frequencies for each cell subset at the indicated time points. Changes, if any, in ABS are described in the text.

noted at week 2 post infection. Levels of ABS returned to near baseline values for the cytolytic $\alpha_4\beta_7$+ CD16+CD56− NK subset by week 5 but remained elevated for $\alpha_4\beta_7$+ CD16+CD56+ NK cells.

With regards to CD4+ T-cells, a steady decline in the frequency of total CD4+ T-cells was observed (Fig. 8B, left panel) and while a 20–30% decrease in the frequency of total $\alpha_4\beta_7$+ CD4+ T-cells and the $\alpha_4\beta_7$+ naïve subset was observed by week 2, no significant changes were noted in the frequency of $\alpha_4\beta_7$+ TCM and $\alpha_4\beta_7$+ TEM subsets (Fig. 8B, right panel). However, the analysis of ABS at week 2 revealed a significant 2–3-fold decline in all three $\alpha_4\beta_7$+ CD4+ T-cell subsets with the largest decrease being observed for $\alpha_4\beta_7$+ naïve and $\alpha_4\beta_7$+ TCM subsets (data not shown). The levels of these subsets remained low with a modest increase in ABS being observed at week 5 post infection. No significant changes in the frequency of $\alpha_4\beta_7$+ CD8+ T-cells and its $\alpha_4\beta_7$+ subsets were observed during the acute infection period (Fig. 8C, right panel). However, in contrast to $\alpha_4\beta_7$+ CD4+ T-cells, a slight increase in the ABS of $\alpha_4\beta_7$+ CD8+ T-cells and its subsets were noted at week 2 post infection, with the largest increase (2-fold) being noted for the $\alpha_4\beta_7$+ TEM subset (data not shown). The ABS of the $\alpha_4\beta_7$+ CD8+ TCM subset remained steady but by weeks 4 and 5, an approximately 2-fold decline in the ABS of the $\alpha_4\beta_7$+ CD8+ naïve and $\alpha_4\beta_7$+ CD8+ TEM subsets were observed. There were no significant changes observed in the frequency of $\alpha_4\beta_7$+ B-cells and there was no clear trend noted in ABS of B-cells during acute SIV-infection (data not shown).

4. Discussion

The implications of $\alpha_4\beta_7$ expression patterns on the ability of distinct cell populations to home to gut mucosal sites have led to efforts to understand both the mechanism behind the substantial decline in CD4+ T-cells in HIV/SIV pathogenesis as well as mechanisms underlying the trafficking of lymphocytes that would naturally replace and potentially help in the control of viral replication at this site of infection. A recent study by Arthos et al. [16] demonstrated that not only was there a direct interaction between $\alpha_4\beta_7$ and the HIV envelope protein gp120 but that depending on the viral isolate, there was considerable variability in the efficiency with which this binding occurred. Thus, in addition to offering one explanation for the rapid decline in mucosal memory CD4+ T-cells during acute HIV infection, these observations also raise the possibility that targeting gp120-$\alpha_4\beta_7$ interactions *in vivo* may interfere with optimal binding, perhaps limiting and/or inhibiting the establishment of a successful viral infection. Studies of *in vivo* blocking studies in mice using antibodies against $\alpha_4\beta_7$ have already laid the foundation for blocking such receptor ligand interactions in the trafficking of T-cells to intestinal tissues [39,40]. Several antagonists for the gut-homing markers $\alpha_4\beta_7$ and even CCR9 are currently in clinical development for the treatment of inflammatory diseases, which include humanized anti-$\alpha_4\beta_7$ antibody and the use of a small molecule CCR9 inhibitor such as Traficet-EN™ (ChemoCentryx) for the treatment of Crohn's disease and ulcera-

tive colitis [41,42]. Exploiting this approach in the context of HIV pathogenesis may prove to be effective since an anti-$\alpha_4\beta_7$ blocking or depleting antibody may have preventative or therapeutic effects. Given the limitations of our knowledge of the potential consequences that such therapy would have in HIV patients, the studies presented herein therefore set out to first characterize $\alpha_4\beta_7$ expression patterns in RM, the non-human primate model of AIDS, and then proceeded to evaluate the safety and efficacy of a Rh-$\alpha_4\beta_7$ mAb which is a recombinant primatized construct of the original murine $\alpha_4\beta_7$ mAb that has previously been shown to specifically recognize the $\alpha_4\beta_7$ heterodimer.

While the analysis of $\alpha_4\beta_7$ expression on various lymphocyte subsets from RM revealed expression patterns that are basically very similar to what has been reported for human lymphocytes, some notable differences were observed. First, $\alpha_4\beta_7$ expression levels on CD8+ T-cells and particularly B-cells in RM were predominantly low which is in contrast to what has been observed on these two lymphocyte subsets in humans. This may possibly be due to a species-specific difference although it should be noted that even in humans, considerable variability in $\alpha_4\beta_7$ density was reported at least for B-cells and this appeared to be age-related [10]. Second, our results showed that $\alpha_4\beta_7^{high}$ is expressed on mostly peripheral CD4+ TCM T-cells (as defined by CD28, CD95 and CCR7 expression) with CD4+ naïve and TEM cells being predominantly $\alpha_4\beta_7^{low}$, and only a small frequency of $\alpha_4\beta_7^{high}$ CD4+ cells were observed in GALT samples which was unexpected. These observations raise the question of whether high densities of $\alpha_4\beta_7$ are truly required for mobilization to the gut or if significant down-regulation of $\alpha_4\beta_7$ expression occurs after $\alpha_4\beta_7$+ lymphocytes have trafficked to this mucosal target site. More detailed trafficking studies of $\alpha_4\beta_7^{low}$ and $\alpha_4\beta_7^{high}$ lymphocytes will be required to better address this issue. Nonetheless, our observation of $\alpha_4\beta_7^{high}$ expression levels on predominantly CD4+ memory T-cells in combination with the recent finding by Arthos et al. regarding the binding of HIV gp120 to $\alpha_4\beta_7$, offers further support for why this cell subset is relatively more susceptible to infection and depletion early in infection. However, our analysis of cellular VL in purified $\alpha_4\beta_7$+ and $\alpha_4\beta_7$– CD4+ T-cell populations from chronically SIV-infected RM suggest no preferential replication of SIV in $\alpha_4\beta_7$+ cells over $\alpha_4\beta_7$– subsets although studies are being pursued by us to determine cellular VL in more specific $\alpha_4\beta_7^{low}$ and $\alpha_4\beta_7^{high}$ subsets, particularly in acutely SIV-infected animals, to elucidate the susceptibility of these cell populations to infection and subsequent depletion. Replacing this depleted population via infusion methods is not implausible as our current study showed that high levels of $\alpha_4\beta_7$ expression on CD4+ T-cells can be effectively induced *in vitro* with RA. Thus, expanding these cells *ex vivo* for possible *in vivo* infusion experiments as a means to replenish CD4+ T-cells and/or provide robust effector CD4+ T-cells that home preferentially to the affected GI compartment is feasible. In support of this, a recent study that involved the *in vivo* tracking of infused CFSE-labeled CD4+ $\alpha_4\beta_7$+ T-cells that were expanded *ex vivo* with anti-CD3/CD28 Abs revealed that the gut tissues contained 2% of such labeled cells at 1 week following infusion (Villinger et al., manuscript in preparation). While results of the *in vitro* RA assay did not reveal any significant induction of $\alpha_4\beta_7$ expression on CD8+ T-cells following a 5-day incubation period with RA, it is possible that the kinetics of $\alpha_4\beta_7$ upregulation on this cell lineage may be delayed in comparison to CD4+ T-cells and prolonged treatment with this Vitamin A metabolite may lead to significant $\alpha_4\beta_7$ induction on CD8+ T-cells.

Our analysis of $\alpha_4\beta_7$ expression in the context of SIV infection revealed rapid peripheral declines in select lymphocyte subsets that include $\alpha_4\beta_7$+ CD4+ T-cells and $\alpha_4\beta_7$+ NK cells primarily during the acute phase. It is not clear whether these rapid peripheral declines in $\alpha_4\beta_7$+ CD4+ T-cells are due to induced trafficking to the GALT, direct cytopathic effects of the virus, or both. Of importance, the declines in peripheral $\alpha_4\beta_7$+ NK cells, particularly within the cytokine-producing $\alpha_4\beta_7$+ CD16–CD56+ subset, suggest that their trafficking to the GI track is induced as early as week 1, setting in motion downstream SIV-specific adaptive immune responses at this major site of infection. In support of this view, a decline in the ABS of $\alpha_4\beta_7$+ naïve and $\alpha_4\beta_7$+ TEM CD8+ T-cells occurred in the periphery at weeks 4 and 5, after the noted decline in $\alpha_4\beta_7$+ CD16–CD56+ NK cells. If trafficking of $\alpha_4\beta_7$+ NK cells to the GALT is indeed occurring, this again raises the question of whether high densities of $\alpha_4\beta_7$ expression are truly required for trafficking to this mucosal site since NK cells in RM were found to exhibit primarily a $\alpha_4\beta_7^{low}$ phenotype, as did CD8+ TEM cells. It is possible that integrins other than $\alpha_4\beta_7$ contribute to trafficking of certain cell lineages to the GI tract. It is of interest to note that there were minimal changes in the level of $\alpha_4\beta_7$+ B-cells during acute SIV infection, suggesting a less prominent role for this cell lineage in the GALT or that other gut-homing receptors are upregulated on B-cells during acute SIV/HIV infection.

Prior to *in vivo* administration of Rh-$\alpha_4\beta_7$ mAb, we confirmed that this mAb had limited immunogenicity to minimize cellular activation that could lead to additional cellular targets for SIV infection therefore counteracting the intended preventive or therapeutic effect of the antibody in future experiments with SIV-infected RM. Experiments to evaluate the effect of this antibody on general tyrosine phosphorylation in unfractionated PBMC or highly enriched population of CD4+ T-cells failed to reveal any detectable increase in phosphorylation when compared to untreated cells (data not shown). An additional *in vitro* ^{3}H-thymidine-based cell proliferation assay revealed that Rh-$\alpha_4\beta_7$ at varying concentrations (0.1–25 μg/ml) failed to induce detectable cell proliferation (data not shown), thus lending further support for the observation that Rh-$\alpha_4\beta_7$ does not induce detectable levels of cell activation at least under these conditions. These data are distinct from a previous study [43] which reported that immobilized $\alpha_4\beta_7$ mAb served to co-stimulate T-cells when used in conjunction with sub-mitogenic doses of anti-CD3 mAb. Similar approaches are therefore being pursued in efforts to determine if in fact our Rh-$\alpha_4\beta_7$ mAb has similar effects. The administration of Rh-$\alpha_4\beta_7$ *in vivo*, even at a high dose of 50 mg/kg was however well tolerated. Importantly, the substantial decline in the frequency and ABS of $\alpha_4\beta_7$+ lymphocytes in both the periphery and GALT on Day 1 suggests that Rh-$v_4\beta_7$ successfully exerted its effect *in vivo*. Although the reduction in ABS and frequency of $\alpha_4\beta_7$+ lymphocytes in the periphery and GALT, respectively, suggests a true decline in these cell populations, the redistribution of these lymphocytes to other compartments cannot be ruled out. For future experiments, it would also be important to determine if such a decrease in ABS also occurs in the GALT following Rh-$\alpha_4\beta_7$ administration.

During the course of this experiment, two additional observations were made which provided important information about both the mAb itself and the nature of the cells that it targets. First, a recovery of β_7 integrin+ lymphocytes was noted in the periphery at Day 5 and thereafter but the level of $\alpha_4\beta_7$+ lymphocytes detected by murine $\alpha_4\beta_7$ mAb was still negligible for >6 weeks after Rh-$\alpha_4\beta_7$ administration, suggesting that circulating Rh-$\alpha_4\beta_7$ cross-blocked newly produced and/or newly trafficking $\alpha_4\beta_7$+ cells upon entry into the periphery thereby blocking their detection by the murine mAb. The finding that the primatized mAb remained in circulation for up to 40–50 days also suggests long-term *in vivo* stability and that it was unlikely that the monkeys generated an immune response to this antibody, which otherwise would have exhibited a faster *in vivo* clearance. Second, our results also revealed that the extent of decline was not uniform among the cell lineages, with a slightly less pronounced decrease being noted for $\alpha_4\beta_7$+ B-cells in the periphery and GALT. It is possible that differences in the tissue

specific redistribution of these cell lineages and/or rates of cell turnover account for this difference, since it has been reported that B-cell turnover in RM occurs at a rate faster than T-cells [44,45]. Thus, the observed lower level of decline of $\alpha_4\beta_7$+ B-cells may be due to quicker neogenesis/replacement of these lymphocytes and perhaps a more substantial decrease may have been observed in the hours immediately following Rh-$\alpha_4\beta_7$ administration. Nonetheless, these data collectively demonstrate that Rh-$\alpha_4\beta_7$ can be safely administered and results in remarkably efficient cross-blocking of the $\alpha_4\beta_7$ receptor and perhaps even a decline due to redistribution and/or depletion of $\alpha_4\beta_7$+ lymphocytes, particularly T-cells which ultimately is the target cell lineage of interest. These observations lay the foundation for future chronic dosing experiments with Rh-$\alpha_4\beta_7$ in acutely and chronically SIV-infected animals. Whether chronic dosing of this mAb leads to safe and sustained cross-blocking, depletion and/or redistribution of $\alpha_4\beta_7$+ lymphocytes remains to be determined and is the current focus of study in our laboratory, as are studies to determine the potential preventative and/or therapeutic effects of Rh-$\alpha_4\beta_7$ during early viral infection.

Acknowledgments

We thank Dr. James T. Kurnick who provided us with the murine $\alpha_4\beta_7$ mAb clone and also thank Stephanie Ehnert and the veterinary and support staff of the YNPRC for their efficient care and handling of the animals. We also thank Ann Mayne, Susan Stephenson, Austin Lewis, Dawn Little and Keli Kolegraff for their help with initial characterization of the murine $\alpha_4\beta_7$ mAb.

Appendix A. Supplementary data

Supplementary data associated with this article can be found, in the online version, at doi:10.1016/j.cellimm.2009.06.012.

References

[1] S. Dandekar, Pathogenesis of HIV in the gastrointestinal tract, Current HIV/AIDS Reports 4 (2007) 10–15.
[2] M. Guadalupe, E. Reay, S. Sankaran, T. Prindiville, J. Flamm, A. McNeil, S. Dandekar, Severe CD4+ T-cell depletion in gut lymphoid tissue during primary human immunodeficiency virus type 1 infection and substantial delay ini restoration following highly active antiretroviral therapy, J. Virol. 77 (2003) 11708–11717.
[3] C. Heise, P. Vogel, C.J. Miller, C.H. Halsted, S. Dandekar, Simian immunideficiency virus infection of the gastrointestinal tract of rhesus macaques. Functional, pathological and morphological changes, Am. J. Pathol. 142 (1993) 1759–1771.
[4] R.P. Johnson, How HIV guts the immune system, N. Engl. J. Med. 358 (2008) 2287–2289.
[5] S. Mehandru, M.A. Poles, K. Tenner-Racz, P. Jean-Pierre, V. Manuelli, P. Lopez, A. Shet, A. Low, H. Mohri, D. Boden, P. Racz, M. Markowitz, Lack of mucosal immune reconstitution during prolonged treatment of acute and early HIV-1 infection, PLoS Med. 3 (2006) 2335–2348.
[6] A.H. Talal, C.E. Irwin, D.T. Dieterich, H. Yee, L. Zhang, Effect of HIV-1 infection on lymphocyte proliferation in gut-associated lymphoid tissue, J. Acquir. Immune. Defic. Syndr. 26 (2001) 208–217.
[7] M. Vajdy, R. Veazey, I. Tham, C. deBakker, S. Westmoreland, M. Neutra, A. Lackner, Early immunologic events in mucosal and systemic lymphoid tissues after intrarectal inoculation with simian immunodeficiency virus, J. Infect. Dis. 184 (2001) 1007–1014.
[8] M. Vajdy, R.S. Veazey, H.K. Knight, A.A. Lackner, M.R. Neutra, Differential effects of simian immunideficiency virus infection on immune inductive and effector sites in the rectal mucosa of rhesus macaques, Am. J. Pathol. 157 (2000) 485–495.
[9] R.S. Veazey, M. DeMaria, L.V. Chalifoux, D.E. Shvetz, D.R. Pauley, H.L. Knight, M. Rosenzweig, R.P. Johnson, R.C. Desrosiers, A.A. Lackner, Gastrointestinal tract as a major site of CD4+ T cell depletion and viral replication in SIV infection, Science 280 (1998) 427–431.
[10] D.J. Erle, M.J. Briskin, E.C. Butcher, A. Garcia-Pardo, A.I. Lazarovits, M. Tidswell, Expression and function of the MAdCAM-1 receptor, integrin $\alpha_4\beta_7$, on human leukocytes, J. Immunol. 153 (1994) 517–527.
[11] J.R. Mora, M.R. Bono, N. Manjunath, W. Weninger, L.L. Cavanagh, M. Rosemblatt, U.H.V. Andrian, Selective imprinting of gut-homing T-cells by Peyer's patch dendritic cells, Nature 424 (2003) 88–93.
[12] L.S. Rott, M.J. Briskin, D.P. Andrew, E.L. Berg, E.C. Butcher, A fundamental subdivision of circulating lymphocytes defined by adhesion to mucosal addressin cell adhesion molecule-1, J. Immunol. 156 (1996) 3727–3736.
[13] T. Schweighoffer, Y. Tanaka, M. Tidswell, D.J. Erle, K.J. Horgan, G.E.G. Luce, A.I. Lazarovits, D. Buck, S. Shaw, Selective expression of integrin $\alpha_4\beta_7$ on a subset of human CD4+ memory T cells with hallmarks of gut-trophism, J. Immunol. 151 (1993) 717–729.
[14] W.W. Agace, T-cell recruitment to the intestinal mucosae, Trends Immunol. 29 (2008) 514–522.
[15] S.I. Hammerschmidt, M. Ahrendt, U. Bode, B. Wahl, E. Kremmer, R. Forster, O. Pabst, Stromal mesenteric lymph node cells are essential for the generation of gut-homing T cells *in vivo*, J. Exp. Med. 205 (2008) 2400–2483.
[16] J. Arthos, C. Cicala, E. Martinelli, K. Macleod, D.V. Ryk, D. Wei, Z. Xiao, T.D. Veenstra, T.P. Conrad, R.A. Lempicki, S. McLaughlin, M. Pascuccio, R. Gopaul, J. McNally, C.C. Cruz, N. Censoplano, E. Chung, K.N. Reitano, S. Kottilil, D.J. Goode, A.S. Fauci, HIV-1 envelope protein binds to and signals through integrin $\alpha_4\beta_7$, the gut mucosal homing receptor for peripheral T cells, Nat. Immunol. 9 (2008) 301–309.
[17] S. Kewenig, T. Schneider, K. Hohloch, K. Lamps-Dreyer, R. Ullrich, N. Stolte, C. Stahl-Hennig, F.J. Kaup, A. Stallmach, M. Zeitz, Rapid mucosal CD4(+) T-cell depletion and enteropathy in simian immunodeficiency virus-infected rhesus macaques, Gastroenterology 116 (1999) 1115–1123.
[18] N.L. Letvin, N.W. King, Immunologic and pathologic manifestations of the infection of rhesus monkeys with simiam immunodeficiency virus of macaques, J. Acqui. Immune. Defic. Syndr. 3 (1990) 1023–1040.
[19] N. Onlamoon, K. Pattanapanyasat, A.A. Ansari, Human and nonhuman primate lentiviral infection and autoimmunity, Ann. NY Acad. Sci. 1050 (2005) 397–409.
[20] P.P. Firpo, I. Axberg, M. Scheibel, E.A. Clark, Macaque CD4+ T-cell subsets: influence of activation on infection by simian immunodeficiency viruses (SIV), AIDS Res. Hum. Retroviruses. 8 (1992) 357–366.
[21] A. Kaur, R.M. Grant, R.E. Means, H. McClure, M. Feinberg, R.P. Johnson, Diverse host responses and outcomes following simian immunodeficiency virus SIVmac239 infection in sooty mangabeys and rhesus macaques, J. Virol. 72 (1998) 9597–9611.
[22] M.R. Reynolds, E. Rakasz, P.J. Skinner, C. White, K. Abel, Z.M. Ma, L. Compton, G. Napoe, N. Wilson, C.J. Miller, A. Haase, D.I. Watkins, CD8+ T-lymphocyte response to major immunodominant epitopes after vaginal exposure to simian immunodeficiency virus: too late and too little, J. Virol. 79 (2005) 9228–9235.
[23] G. Silvestri, A. Fedanov, S. Germon, N. Kozyr, W.J. Kaiser, D.A. Garber, H. McClure, M.B. Feinberg, S.I. Staprans, Divergent host responses during primary simian immunodeficiency virus SIVsm infection of natural sooty mangabey and nonnatural rhesus macaque hosts, J. Virol. 79 (2005) 4043–4054.
[24] R.S. Veazey, I.C. Tham, K.G. Mansfield, M. DeMaria, A.E. Forand, D.E. Shvetz, L.V. Chalifoux, P.K. Sehgal, A.A. Lackner, Identifying the target cell in primary simian immunodeficiency virus (SIV) infection: highly activated memory CD4(+) T cells are rapidly eliminated in early SIV infection *in vivo*, J. Virol. 74 (2000) 57–64.
[25] A.A. Lackner, R.S. Veazey, Current concepts in AIDS pathogenesis: insights from the SIV-macaque model, Annu. Rev. Med. 58 (2007) 461–476.
[26] A.I. Lazarovits, R.A. Moscicki, J.T. Kurnik, D. Camerini, A.K. Bhan, L.G. Baird, M. Erikson, R.B. Colvin, Lymphocyte activation antigens: A monoclonal antibody, anti-Act1, defines a new late lymphocyte activation antigen, J. Immunol. 133 (1984) 1857–1862.
[27] M.J. Benson, K. Pino-Lagos, M. Rosemblatt, R.J. Noelle, All-trans retinoic acid mediates enhanced T reg cell growth, differentiation, and gut homing in the face of high levels of co-stimulation, J. Exp. Med. 204 (2007) 1765–1774.
[28] J.L. Coombes, K.R.R. Siddiqui, C.V. Arancibia-Carcamo, J. Hall, C.-M. Sun, Y. Belkaid, F. Powrie, A functionally specialized population of CD103+ DCs induces FoxP3+ regulatory T cells via a TGF-β- and retinoic acid-dependent mechanism, J. Exp. Med. 204 (2007) 1757–1764.
[29] M. Iwata, A. Hirakiyama, Y. Eshima, H. Kagechika, C. Kato, S.Y. Song, Retinoic acid imprints gut-homing specificity on T cells, Immunity 21 (2004) 458–466.
[30] B. Johansson-Lindbom, M. Svensson, O. Pabst, C. Palmqvist, G. Marquez, R. Förster, W.W. Agace, Functional specialization of gut CD103+ dendritic cells in the regulation of tissue-selective T cell homing, J. Exp. Med. 202 (2005) 1063–1073.
[31] S.G. Kang, H.W. Lim, O.M. Andrisani, H.E. Broxmeyer, C.H. Kim, Vitamin A metabolites induce gut-homing FoxP3+ regulatory T cells, J. Immunol. 179 (2007) 3724–3733.
[32] A.J. Stagg, M.A. Kamm, S.C. Knight, Intestinal dendritic cells increase T cell expression of alpha4beta7 integrin, Eur. J. Immunol. 32 (2002) 1445–1454.
[33] N.R. Klatt, F. Villinger, P. Bostik, S.N. Gordon, L. Pereira, J.D. Estes, J.C. Engram, A. Mayne, R.M. Dunham, B. Lawson, D.L. Sodora, S.I. Staprans, K. Reimann, G. Silvestri, A.A. Ansari, The availability of activated CD4+ T cells is a major determinant of set point viremia during natural SIV infection of sooty mangabeys, J. Clin. Invest. 118 (2008) 2039–2049.
[34] L.E. Pereira, R.P. Johnson, A.A. Ansari, Sooty mangabeys and rhesus macaques exhibit significant divergent natural killer cell responses during both acute and chronic phases of SIV infection, Cell Immunol. 254 (2008) 10–19.
[35] F. Villinger, G.T. Brice, A.E. Mayne, P. Bostik, K. Mori, C.H. June, A.A. Ansari, Adoptive transfer of simian immunodeficiency virus (SIV) naive autologous CD4+ cells to macaques chronically infected with SIV is sufficient to induce long-term nonprogressor status, Blood 99 (2002) 590–599.

[36] J.M. Bator, C.L. Reading, Measurement of antibody affinity for cell surface antigens using an enzyme linked immunosorbent assay, J. Immunol. Meth. 125 (1989) 167–176.
[37] M.A. Cromwell, R.S. Veazey, J.D. Altman, K.G. Mansfield, R. Glickman, T.M. Allen, D.I. Watkins, A.A. Lackner, R.P. Johnson, Induction of mucosal homing virus-specific CD8+ T lymphocytes by attenuated simian immunodeficiency virus, J. Virol. 74 (2000) 8762–8766.
[38] D.T. Evans, L.M. Chen, J. Gillis, K.C. Lin, B. Harty, G.P. Mazzara, R.O. Donis, K.G. Mansfield, J.D. Lifson, R.C. Desrosiers, J.E. Galan, R.P. Johnson, Mucosal priming of simian immunodeficiency virus-specific cytotoxic T-lymphocyte responses in rhesus macaques by the Salmonella type III secretion antigen delivery system, J. Virol. 77 (2003) 2400–2409.
[39] S.R. Reese, K.A. Kudsk, L. Genton, S. Ikeda, L-selectin and alpha4beta7 integrin, but not ICAM-1, regulate lymphocyte distribution in gut-associated lymphoid tissue of mice, Surgery 137 (2005) 209–215.
[40] M.A. Wurbel, M. Malissen, D. Guy-Grand, E. Meffre, M.C. Nussenzweig, M. Richelme, A. Carrier, B. Malissen, Mice lacking the CCR9 CC-chemokine receptor show a mild impairment of early T- and B-cell development and a reduction in T-cell receptor gammadelta(+) gut intraepithelial lymphocytes, Blood 98 (2001) 2626–2632.
[41] B.G. Feagan, G.R. Greenberg, G. Wild, R.N. Fedorak, P. Paré, J.W. McDonald, A. Cohen, A. Bitton, J. Baker, R. Dubé, S.B. Landau, M.K. Vandervoort, A. Parikh, Treatment of active Crohn's disease with MLN0002, a humanized antibody to the alpha4beta7 integrin, Clin. Gastroenterol. Hepatol. 6 (2008) 1370–1377.
[42] B.G. Feagan, G.R. Greenberg, G. Wild, R.N. Fedorak, P. Pare, J.W. McDonald, R. Dube, A. Cohen, A.H. Steinhart, S. Landau, R.A. Aguzzi, I.H. Fox, M.K. Vandervoort, Treatment of ulcerative colitis with a humanized antibody to the alpha4beta7 integrin, N. Engl. J. Med. 352 (2005) 2499–2507.
[43] T.K. Teaugue, A.I. Lazarovits, B.W. McIntyre, Integrin alpha4beta7 co-stimulation of human peripheral blood T cell proliferation, Cell Adhes. Commun. 2 (1994) 539–547.
[44] R.J.D. Boer, H. Mohri, D.D. Ho, A.S. Perelson, Turnover rates of B cells, T cells, and NK cells in simian immunodeficiency virus-infected and uninfected rhesus macaques, J. Immunol. 170 (2003) 2479–2487.
[45] H. Mohri, S. Bonhoeffer, S. Monard, A.S. Perelson, D.D. Ho, Rapid turnover of T lymphocytes in SIV-infected rhesus macaques, Science 279 (1998) 1223–1227.

Biochemical and Biophysical Research Communications 380 (2009) 838–843

Contents lists available at ScienceDirect

Biochemical and Biophysical Research Communications

journal homepage: www.elsevier.com/locate/ybbrc

Inhibition of human immunodeficiency virus type 1 (HIV-1) nuclear import via Vpr–Importin α interactions as a novel HIV-1 therapy

Tatsunori Suzuki [a], Norio Yamamoto [a,b], Mizuho Nonaka [a], Yoshie Hashimoto [a], Go Matsuda [a], Shin-nosuke Takeshima [a], Megumi Matsuyama [c], Tatsuhiko Igarashi [c], Tomoyuki Miura [c], Rie Tanaka [d], Shingo Kato [d], Yoko Aida [a,*]

[a] Viral Infectious Diseases Unit, RIKEN, 2-1 Hirosawa, Wako, Saitama 351-0198, Japan
[b] Department of General Medicine, Juntendo University School of Medicine, 2-1-1 Hongo, Bunkyo-ku, Tokyo 113-8421, Japan
[c] Institute for Virus Research, Kyoto University, Kyoto 606-8507, Japan
[d] Department of Microbiology and Immunology, Keio University School of Medicine, 35 Shinanomachi, Shinjyuku-ku, Tokyo 160-8582, Japan

ARTICLE INFO

Article history:
Received 18 January 2009
Available online 4 February 2009

Keywords:
HIV-1 inhibitor
Vpr
Nuclear import inhibition
Importin α
Small molecule
Macrophage

ABSTRACT

The development of multidrug-resistant viruses compromises the efficacy of anti-human immunodeficiency virus (HIV) therapy and limits treatment options. Therefore, new targets that can be used to develop novel antiviral agents need to be identified. One such target is the interaction between Vpr, one of the accessory gene products of HIV-1 and Importin α, which is crucial, not only for the nuclear import of Vpr, but also for HIV-1 replication in macrophages. We have identified a potential parent compound, hematoxylin, which suppresses Vpr–Importin α interaction, thereby inhibiting HIV-1 replication in a Vpr-dependent manner. Analysis by real-time PCR demonstrated that hematoxylin specifically inhibited nuclear import step of pre-integration complex. Thus, hematoxylin is a new anti-HIV-1 inhibitor that targets the nuclear import of HIV-1 via the Vpr–Importin α interaction, suggesting that a specific inhibitor of the interaction between viral protein and the cellular factor may provide a new strategy for HIV-1 therapy.

Macrophages are a major target of human immunodeficiency virus type 1 (HIV-1) and serve as a viral reservoir for the release of small amounts of viral particles in symptomatic carriers [1]. HIV-1 in latently infected macrophages in some lymphoreticular tissues cannot be eradicated by highly active anti-retroviral therapy (HAART), and these cells may produce viral particles that can spread throughout the body [2]. A striking feature of HIV-1 is its ability to replicate in non-dividing cells, in particular, macrophages. Replication in non-dividing cells depends on the active nuclear import of the viral pre-integration complex (PIC) [3]. The HIV-1 PIC exhibits biophysical properties typical of a large nucleo–protein complex and contains the viral proteins reverse transcriptase, integrase (IN), nucleocapsid, Vpr, and small amounts of matrix (MA), in addition to the viral nucleic acids [4–7]. Three PIC-associated proteins, MA, IN, and Vpr, have been proposed as karyophilic agents that act probably via their interactions with Importin (Imp) α, Imp β, and/or Imp 7 [8]. In addition, a recent study indicates that transportin-SR2, which shuttles the essential splicing factor, mediates PIC nuclear import, thereby facilitating HIV infection [9]. Moreover, a novel partner, tRNA, has been shown to facilitate PIC nuclear import [10]. However, the molecular mechanisms of PIC nuclear import and its role in viral replication in macrophages are still not completely understood.

Several studies have shown that Vpr is essential for the nuclear import of PIC in macrophages [11,12], while others do not support such observations [13]. However, our studies have clearly shown that Vpr is targeted to the nuclear envelope and then transported into the nucleus by Imp α alone, in an Imp β-independent manner [12,14]. Furthermore, the interaction between Imp α and the N-terminal α-helical domain (αH1) of Vpr, amino acid residues 17–34, is indispensable, not only for nuclear import of Vpr, but also for HIV-1 replication in macrophages [12]. Thus, it appears that Vpr–Imp α binding precedes a novel nuclear import process, which is a potential target for therapeutic intervention in macrophages, which is crucial for subsequent viral spread to lymphoid organs and T-helper lymphocytes [15]. In addition to nuclear transport, Vpr also has other important functions, including the induction of cell cycle arrest at the G_2 phase [16], the regulation of apoptosis [16,17] and splicing [18,19], carried out through interactions with a variety of cellular partners. These observations suggest that drug targeting of Vpr may lead to pleiotropic effects on the HIV life cycle.

As a promising target for blocking HIV-1 replication in macrophages, by screening a large collection of chemical compounds,

* Corresponding author. Fax: +81 48 462 4399.
E-mail address: aida@riken.jp (Y. Aida).

0006-291X/$ - see front matter © 2009 Elsevier Inc. All rights reserved.
doi:10.1016/j.bbrc.2009.01.180

we here discovered several compounds that selectively inhibit the nuclear import of Vpr in an Imp α-dependent manner. Importantly, hematoxylin blocks HIV-1 replication in a Vpr-dependent manner in macrophages by blocking the nuclear import of PIC, but does not block Vpr-induced G_2 cell cycle arrest, the virion incorporation function of Vpr and nuclear import of karyophilins, which possess the classical nuclear localization signal (cNLS).

Materials and methods

Enzyme linked immuno-sorbent assay (ELISA)-based binding assay. The wells of 96-well microplates (NUNC) were coated with an anti-glutathione *S*-transferase (GST)-specific monoclonal antibodies (MAb) (Sigma) in 50 mM $NaHCO_3$ (pH 9.8) for 6 h at 4 °C. After washing the wells, GST or GST-N17C74 (0.5 μg/well) in phosphate-buffered saline (PBS) containing 5% bovine serum albumin (BSA) were added to the wells and incubated for 2 h at 4 °C. Imp α-histidine tag_6 (His_6) was added to the wells together with Imp β or test compounds and incubated for 2 h at 4 °C. The horseradish peroxidase (HRP)-conjugated anti-His tag MAb (Sigma) was added. Following incubation at 22 °C for 1 h, the microplates were washed three times and tetramethylbenzidine (TMB) (Pierce) was added. After incubation at 37 °C for 30 min, the amount of surface-bound Imp α was estimated by monitoring the optical density of the wells at 450 nm using an ELISA plate reader (Wallac ARVO™ SX 1420; Perkin-Elmer).

Viral infection assay. Primary macrophages in 24-well plates were inoculated with vesicular stomatitis virus G (VSV-G) pseudotyped reporter virus [NL-Luc-E^-R^+ (VSV-G) or NL-Luc-E^-R^- (VSV-G); 4 ng of p24 antigen], cultured in the absence or presence of hematoxylin for 2 days, harvested, and lysed in luciferase assay substrate (Promega). Luciferase activity was measured using a Wallac ARVO™ SX 1420 luminometer (Perkin-Elmer). Moreover, primary macrophages were exposed to diluted virus stocks (containing 2 or 20 ng of p24 antigen), the JR-CSF strain of the HIV-1 macrophage-tropic virus for 3 h at 37 °C. The cells were then washed three times and seeded in a 24-well tissue-culture plate (NUNC) for primary macrophages. Cells were maintained in RPMI-1640 that contained 10% fetal calf serum. Culture supernatants were harvested at 4-, 8-, 12-, 16-day intervals for primary macrophages and viral production was monitored by sequential quantitation of p24 antigen in cell-free supernatants using an HIV-1 $p24^{gag}$ ELISA kit (LUMIPULSE; Fuji REBIO).

Quantitative real-time PCR. Real-time PCR for quantification of total viral DNA, 2-long terminal repeat (LTR) circular DNA, was performed as follows. Differentiated primary macrophages were infected with VSV-G pseudotyped reporter viruses [NL-Luc-E^-R^+ (VSV-G) or NL-Luc-E^-R^- (VSV-G)] containing 4 ng of p24 antigen and genomic DNA was isolated at 24 h. Total DNA, 2-LTR DNA, and β-globin were quantified with specific primers (2-LTR-forward, ccctcagacccttttagtcagtg; 2-LTR-reverse, tggtgtgtagttctgccaatca; U5gag forward, gtagtgtgtgcccgtctgttg; U5gag reverse, caagccgagtcctgcgt; β-globin primers were those used by Yamamoto et al. [20]).

Other assays. Other assays were described in Supplementary materials.

Results

To identify compounds inhibiting HIV-1 replication, we focused on the nuclear entry of HIV-1 via the Vpr–Imp α interaction as a target for therapeutic strategies and performed ELISA-based binding assays using natural product libraries derived from microbial and fungal metabolites. For these experiments, we used the Vpr N17C74 fragment (containing residues 17–74), because this is a functionally transportable region [12,14]. Among 49 compounds that specifically inhibited the interaction between N17C74 and Imp α, as measured by the ELISA-based binding assay (Fig. 1B), one compound, hematoxylin, inhibited specific binding of Vpr to Imp α in a dose-dependent manner, as assessed by *in vitro* pull-down assays (Fig. 1A and C). Next, we tested the effect of this compound in an *in vitro* nuclear import assay using digitonin-permeabilized HeLa cells. Interestingly, Imp α-mediated nuclear import of Vpr was dose-dependently inhibited by the addition of hematoxylin with a mean 50% inhibitory concentration (IC_{50}) of 5 μM, suggesting that hematoxylin is a potent small-molecule inhibitor of Vpr nuclear entry. Furthermore, we demonstrated the effect of hematoxylin on Vpr-mediated G_2 phase cell cycle arrest, which is one of the major roles of Vpr in HIV-1 replication (Fig. 2B). Flow-cytometry analysis showed that hematoxylin failed to inhibit the Vpr-induced G_2 phase cell cycle arrest. The αH1 which is essential for the nuclear import of Vpr appeared to be critical for the expression, stability and incorporation of Vpr into the viral particle [14,21]. Therefore, we analyzed whether hematoxylin has an effect on the incorporation of Vpr into viral particle using the virion incorporation assay. Hematoxylin had no effect on the virion incor-

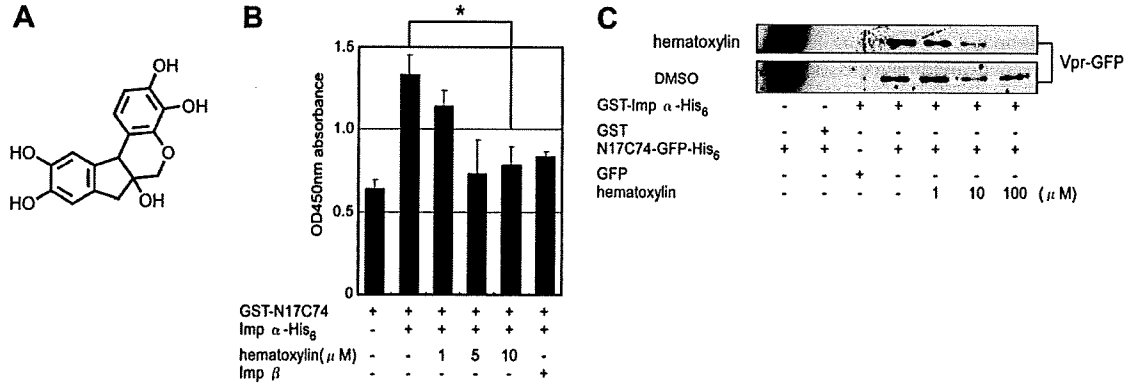

Fig. 1. Identification of a small-molecule that inhibits the interaction between Vpr and Imp α. (A) Chemical structure of hematoxylin. (B) Binding of GST-N17C74 to Imp α-His_6 was quantified using an ELISA-based binding assay. The bound GST-N17C74 was incubated with Imp α-His_6 in the absence (−) or presence (+) of Imp β or hematoxylin. Bound Imp α-His_6 was detected using a HRP-conjugated anti-His MAb. The data are presented as means ± standard deviation of three independent experiments. The asterisk (*) indicates a statistically significant difference ($p < 0.05$). (C) Glutathione-Sepharose beads coupled with GST–Imp α-His_6 or GST were incubated with N17C74-green fluorescence protein (GFP)-His_6 or GFP in the absence (−) or presence of 1, 10 or 100 μM hematoxylin, or 1, 10 or 100 μl dimethyl sulfoxyde (DMSO). The bound fractions were analyzed by Western blotting with anti-GFP MAb.

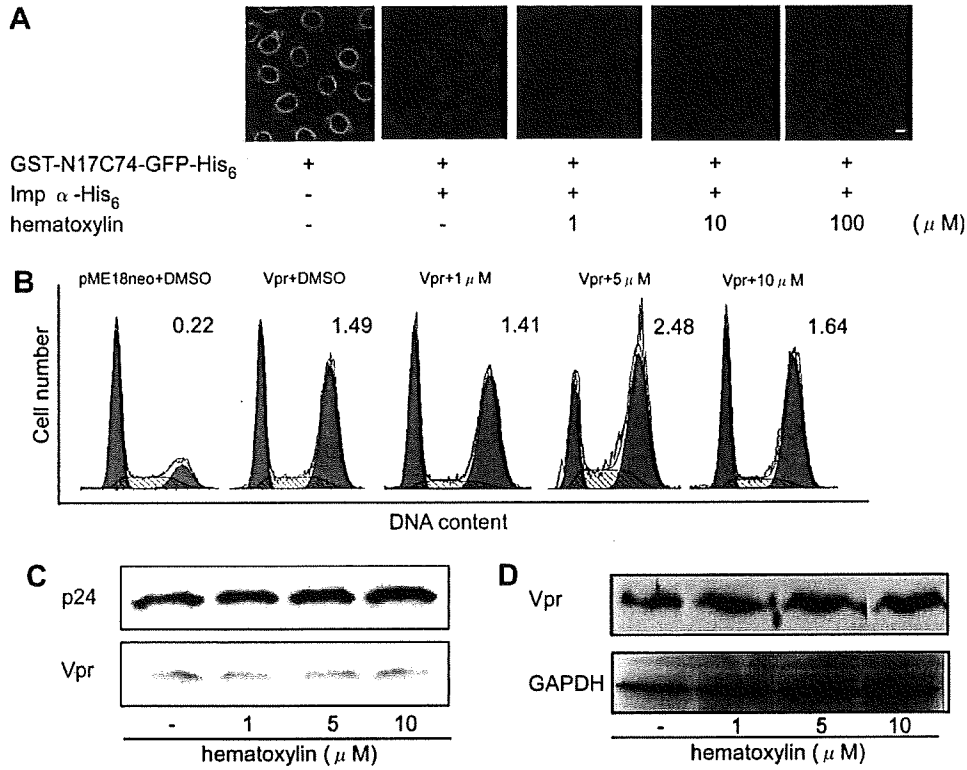

Fig. 2. Hematoxylin inhibits the nuclear import of Vpr by Imp α. (A) Nuclear import of Vpr by Imp α. Digitonin-permeabilized HeLa cells were incubated with 1 μM of GST-N17C74-GFP-His_6 in the absence (−) or presence (+) of 2 μM Imp α, or the indicated concentration of hematoxylin. After fixation, cells were analyzed by confocal laser-scanning microscopy. Bar = 10 μm. (B) Vpr-mediated G_2 arrest. HeLa cells were transfected with pME18Neo encoding Flag-tagged Vpr, or the pME18Neo-Flag, together with pEGFP-N1. At 42 h after addition of 1, 5 or 10 μm hematoxylin, cells were fixed and stained with propidium iodide (PI) for analysis of DNA content and GFP-positive cells were analyzed by flow-cytometry. The proportion of cells in the G_2 phase is indicated at the upper right in each panel. (C) Incorporation of Vpr into viral particles. At 6 h post transfection with pNL4-3, 293T cells were cultured in the absence or presence of hematoxylin, and viral particles were analyzed by Western blotting with anti-Vpr antibody or anti-HIV-1 p24 MAb. (D) Stability of Vpr in HeLa cells. At 6 h post transfection with pME18Neo encoding Flag-tagged Vpr, HeLa cells were cultured in the absence or presence of hematoxylin cells were harvested, lysed and analyzed by Western blotting with anti-Flag M2 MAb and anti-GAPDH MAb.

poration function of Vpr (Fig. 2C). As regards the stability of Vpr, Western blotting analysis showed that the expression level of Vpr in HeLa cells was not affected by hematoxylin 48 h post transfection (Fig. 2D). These results clearly indicate that although hematoxylin has a specific effect on the nuclear import of Vpr, it does not affect the ability of the Vpr to induce G_2 cell cycle arrest or the virion incorporation function of Vpr.

Given the key role played by Vpr in the nuclear import of PIC in non-dividing cells, treatment of infected macrophages with hematoxylin might block HIV-1 replication. Initial experiments were designed to determine a concentration of hematoxylin that could be used with minimal effects on cell viability and cell cycle progression. We investigated the survival of hematoxylin treated human primary macrophages. Macrophages were incubated with hematoxylin at various concentrations in complete culture medium for 15 days and cell viability was evaluated using a 3-(4, 5-dimethylthylthiazol-2-yl)-2, 5-diphenyltetrazolium bromide (MTT) assay (Fig. 3A). For primary macrophages, hematoxylin was toxic with a 50% cytotoxity concentration (CC_{50}) of >40 μM, respectively. Hematoxylin had no effect on the host cell cycle progression, as indicated by flow-cytometry analysis (Fig. 3B). Given the results here, hematoxylin had no adverse effect on the cell growth and viability of the cells at the IC_{50} concentrations for the binding and nuclear import assays, determined in Figs. 1 and 2. Furthermore, we tested whether nuclear import of the cNLS, which requires the formation of a ternary complex of Imp β and Imp α, was inhibited by hematoxylin. The cNLS-Imp α interaction and classical transport were not inhibited by hematoxylin (Fig. 3C and D), implying that hematoxylin has a specific action on the Imp α-mediated nuclear import of Vpr.

Vpr is essential for the nuclear import of PIC in macrophages. Therefore, specific inhibition of nuclear import by hematoxylin via the Vpr–Imp α interaction led us to investigate whether hematoxylin blocks HIV-1 replication in macrophages. Primary macrophages were infected with the macrophage-tropic JR-CSF HIV-1 strain at low viral input (2 ng of p24 antigen) and cultured for 8 days in the presence or absence of hematoxylin at indicated concentrations (Fig. 4A, left panel). Virus replication was monitored at 4 or 8 days post infection by p24 ELISA. Hematoxylin blocked virus replication efficiently and in a dose-dependent manner, reaching inhibition levels up to about 50% and 70% in 4 and 8 days, respectively, at 20 μM (IC_{50} = 1.64 μM). Similarly, results of infection at high viral input (20 ng of p24 antigen) showed same tendency (Fig. 4A, right panel). Furthermore, to confirm the effect of hematoxylin on HIV-1 replication in macrophages, macrophages were infected with a VSV-G-pseudotype HIV-1 strain that encoded either the wild-type Vpr or a truncated Vpr which can only support a single round of HIV-1 replication, and cultured for 2 days in the absence or presence of 2.5, 5, 10 or 20 μM hematoxylin (Fig. 4B). When hematoxylin was added at the time of infection, the replication of Vpr^+ virus was suppressed by hematoxylin in a dose-dependent manner with a mean of IC_{50} of 5 μM (Fig. 4B). Importantly, levels of luciferase activity of the Vpr^- virus were not effective in each concentration of hematoxylin, indicating that inhibition of viral replication by hematoxylin is a Vpr-dependent manner.

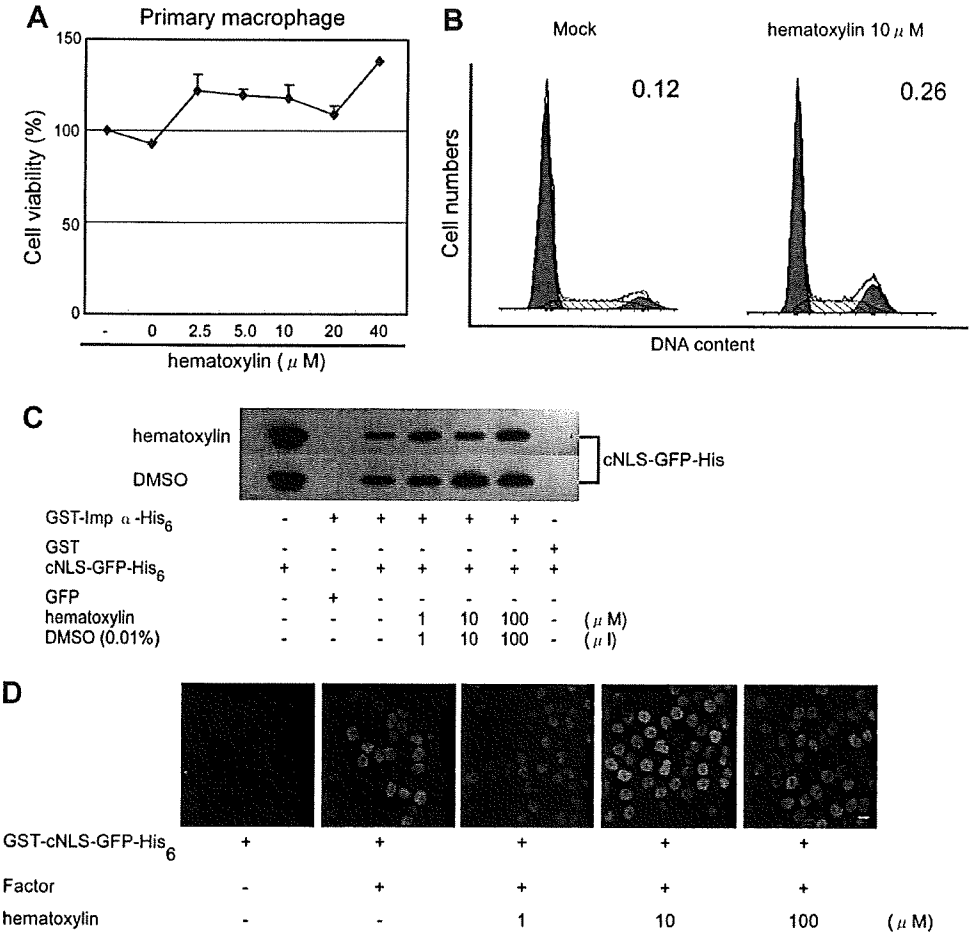

Fig. 3. Analysis of the effect of hematoxylin on normal cell functions. (A) Differentiated primary macrophages were treated with the indicated concentrations of hematoxylin for 15 days. Cell viability was determined using an MTT assay. (B) HeLa cells were treated with 10 μM hematoxylin for 48 h and cell cycle profiles were analyzed by flow cytometry. (C) Glutathione-Sepharose beads coupled with GST–Imp α-His_6 or GST were incubated with cNLS-GFP-His_6 or GFP as a control, in the absence (–) or presence of hematoxylin or DMSO at indicated concentrations. The bound fractions were analyzed by Western blotting with a GFP-specific MAb. (D) Digitonin-permeabilized HeLa cells were incubated with GST-cNLS-GFP-His_6 in the absence (–) or presence (+) of hematoxylin and soluble factors as described previously [12], and then analyzed by confocal laser-scanning microscopy. Bar = 10 μm.

To determine the target of hematoxylin in HIV-1 life cycle, we quantified the viral nucleic acid species present in macrophages after infection. We analyzed the effect of hematoxylin on the formation of late reverse transcripts, as an indicator of total viral DNA (U5 gag as shown in the text), 2-LTR circular DNA, as a marker for successful nuclear import of viral genomic DNA [22]. Treatment with hematoxylin dramatically reduced the amount of 2-LTR circular forms without affecting the copy numbers of U5 gag total DNA in a Vpr-dependent manner (Fig. 4C). These results strongly indicate that the anti-retroviral activity of hematoxylin is likely to be mediated by inhibition of HIV-1 nuclear transport, in macrophages, rather than other steps, such as virus entry and virus maturation.

Discussion

In this study, we explored the anti-HIV activity of hematoxylin, a compound screened by ELISA-binding assays to target the interaction between Vpr and Imp α. By targeting the Vpr–Imp α interaction, we successfully identified a compound inhibiting HIV-1 replication. This result indicates that a specific inhibitor of an interaction between a viral protein and a host cellular factor may provide a new therapeutic strategy for blocking HIV-1 replication. Our results further demonstrate that hematoxylin can efficiently block the nuclear import of Vpr and PIC, and potently blocked HIV-1 replication with Vpr-dependent manner in macrophages. By contrast, hematoxylin, did not inhibit HIV-1 replication in peripheral blood mononuclear cells (PBMCs), which limits the effectiveness of nuclear import inhibitors (unpublished data). This result strongly suggests that Vpr–Imp α interaction is a valuable new drug target which can be exploited for the development of HIV-1 therapies targeting macrophages which cannot be eradicated by HAART.

In present study, by targeting the interaction between Imp α and αH1, we identified a compound inhibiting HIV-1 replication. However, whether hematoxylin directly interacts with Imp α or Vpr remains to be clarified. Recently, using a new hematoxylin derivative and photo-cross-linked small-molecule affinity matrix assay, we obtained evidence to suggest that hematoxylin derivative directly interacts with the αH1 domain of Vpr, but does not interact with Imp α (unpublished data). We postulate that hematoxylin directly bind αH1 and that specifically inhibit Vpr–Imp α interaction without disrupting the global structure of Vpr, because hematoxylin did not inhibit the incorporation of Vpr into viral particle, which is mediated by the αH1 domain. Moreover, the modified Wu-Kabat variability index clearly showed that the αH1 of Vpr is highly conserved among various HIV-1 strains, compared to the

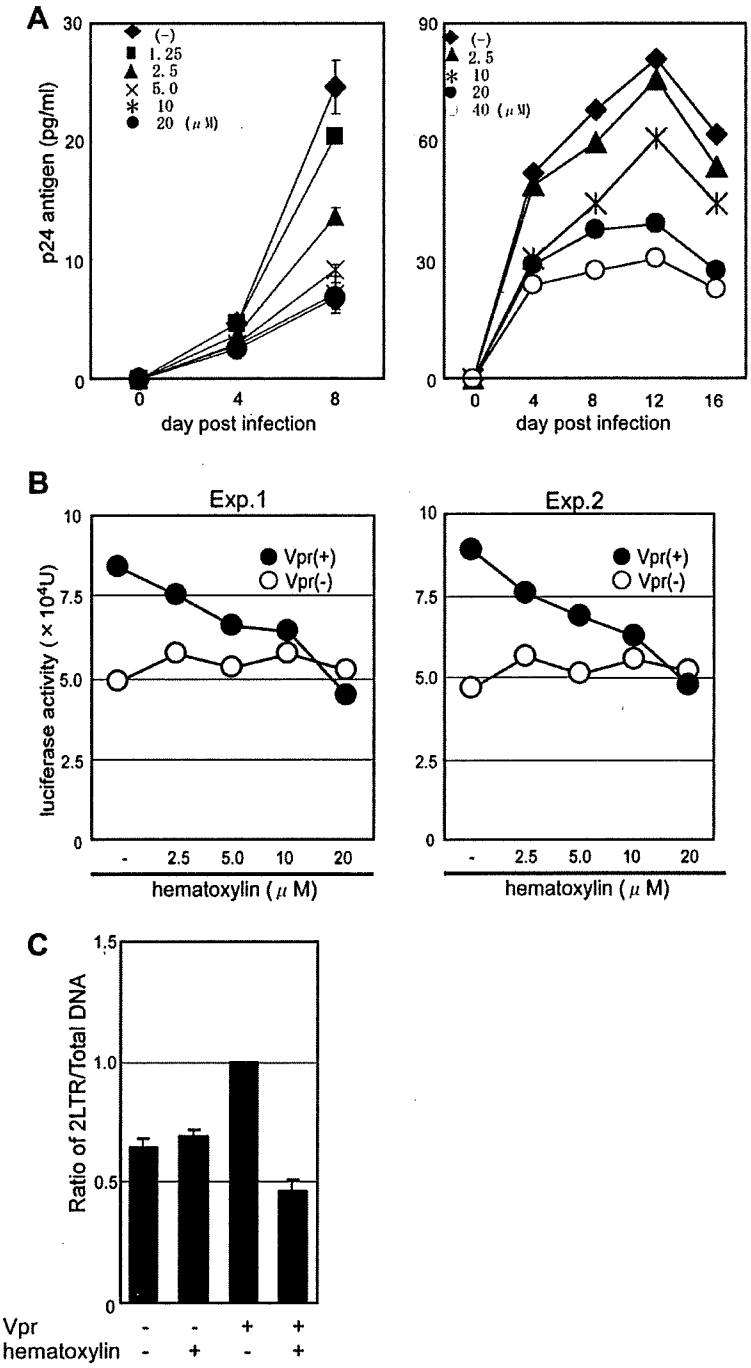

Fig. 4. Hematoxylin inhibition of HIV-1 replication depends on the Vpr in macrophages. (A) Macrophages were infected with HIV-1 (JR-CSF strain) at 2 ng (left panel) or 20 ng (right panel) of p24 antigen in the absence or presence of hematoxylin. Cells were maintained for 4, 8, 12 and 16 days, and the levels of virus production in the culture supernatants were measured by p24 antigen ELISA. (B) Macrophages from two healthy donors were infected with VSV-G-pseudotype virus encoded wild-type Vpr (closed circle) or truncated Vpr (open circle) at 4.0 ng of p24 antigen, and cultured in the absence or presence of hematoxylin. Proviral gene expression was analyzed by luciferase assays 2 days after the infection. (C) Macrophages were infected with the VSV-G-pseudotype virus encoding wild-type Vpr or truncated Vpr at 4 ng of p24 antigen and cultured in the absence or presence of 10 μM hematoxylin. Total HIV-1 DNA and 2-LTR DNA were determined using real-time PCR at 24 h post infection. All samples were tested in duplicate or triplicate, and the data are presented the mean levels of p24 antigen or luciferase activity.

α-helix 2 and α-helix 3 domains, suggesting that the αH1 domain may play crucial roles in HIV-1 survival (unpublished data). Although these data are preliminary, the fact that hematoxylin directly binds to αH1 predicts that HIV-1 resistance to hematoxylin would occur far less frequently than resistance to other conventional drugs. More importantly, understanding of the detailed mechanism of the interaction between Vpr and hematoxylin is essential.

Three HIV-1 proteins, Vpr, MA, and IN, have been proposed as karyophilic agents that recruit the cellular nuclear import machin-

ery to the PIC [8]. Other machineries in addition to the Vpr likely contribute to HIV-1 nuclear import; nevertheless, potent inhibition of HIV-1 replication was achieved by hematoxylin inhibition of Vpr–Imp α interaction. As shown in Fig. 4A, although hematoxylin blocked viral replication efficiently, resulting in 70% on 8 or 16 day, it did not block viral replication completely. This may indicate that there are PIC nuclear import pathways that mediate PIC nuclear import independently of the Vpr; for example, Imp β, Imp 7, Imp β/Imp 7 heterodimer and transportin-SR2 are involved in the nuclear import of PIC into macrophages. In addition, IN, MA, and Vpr either work sequentially or synergistically to regulate PIC nuclear import.

Our results demonstrate that the Vpr–Imp α interaction, a virus protein–cellular protein interaction, is a potential target for an antiviral agent that inhibits nuclear entry. To clarify the mechanism of action of hematoxylin, we are conducting ongoing studies to analyze the crystal structures of the hematoxylin–αH1 domain complex and the αH1 domain–Imp α complex. Detailed descriptions of these interactions will provide new therapeutic strategies for rational drug design. Nuclear import-blocking drugs may be useful not only against HIV, but also against other viruses that require nuclear import for replication, such as the influenza virus, hepatitis B virus, or herpes viruses. The development of such compounds is likely to provide a valuable enrichment of our arsenal of antiviral drugs.

Acknowledgments

We thank Drs. K. Tokunaga, A. Koito, and K. Strebel for kindly providing VSV-G pseudotyped reporter viruses and anti-Vpr antibody. This work was supported in part by a Health Sciences Research Grant from the Ministry of Health, Labor and Welfare of Japan (Research on HIV/AIDS), by the program for Promotion of Fundamental Studies in Health Sciences of the National Institute of Biomedical Innovation (NIBIO) of Japan, and by the Chemical Biology Research Project (RIKEN).

Appendix A. Supplementary data

Supplementary data associated with this article can be found, in the online version, at doi:10.1016/j.bbrc.2009.01.180.

References

[1] J.M. Orenstein, C. Fox, S.M. Wahl, Macrophages as a source of HIV during opportunistic infections, Science 276 (1997) 1857–1861.
[2] J.M. Orenstein, M. Feinberg, C. Yoder, L. Schrager, J.M. Mican, D.J. Schwartzentruber, R.T. Davey Jr., R.E. Walker, J. Falloon, J.A. Kovacs, K.D. Miller, C. Fox, J.A. Metcalf, H. Masur, M.A. Polis, Lymph node architecture preceding and following 6 months of potent antiviral therapy: follicular hyperplasia persists in parallel with p24 antigen restoration after involution and CD4 cell depletion in an AIDS patient, AIDS 13 (1999) 2219–2229.
[3] M.I. Bukrinsky, N. Sharova, M.P. Dempsey, T.L. Stanwick, A.G. Bukrinskaya, S. Haggerty, M. Stevenson, Active nuclear import of human immunodeficiency virus type 1 preintegration complexes, Proc. Natl. Acad. Sci. USA 89 (1992) 6580–6584.
[4] M.I. Bukrinsky, S. Haggerty, M.P. Dempsey, N. Sharova, A. Adzhubel, L. Spitz, P. Lewis, D. Goldfarb, M. Emerman, M. Stevenson, A nuclear localization signal within HIV-1 matrix protein that governs infection of non-dividing cells, Nature 365 (1993) 666–669.
[5] C.M. Farnet, W.A. Haseltine, Determination of viral proteins present in the human immunodeficiency virus type 1 preintegration complex, J. Virol. 65 (1991) 1910–1915.
[6] A. Fassati, S.P. Goff, Characterization of intracellular reverse transcription complexes of human immunodeficiency virus type 1, J. Virol. 75 (2001) 3626–3635.
[7] M.D. Miller, C.M. Farnet, F.D. Bushman, Human immunodeficiency virus type 1 preintegration complexes: studies of organization and composition, J. Virol. 71 (1997) 5382–5390.
[8] J. De Rijck, L. Vandekerckhove, F. Christ, Z. Debyser, Lentiviral nuclear import: a complex interplay between virus and host, Bioessays 29 (2007) 441–451.
[9] F. Christ, W. Thys, J. De Rijck, R. Gijsbers, A. Albanese, D. Arosio, S. Emiliani, J.C. Rain, R. Benarous, A. Cereseto, Z. Debyser, Transportin-SR2 imports HIV into the nucleus, Curr. Biol. 18 (2008) 1192–1202.
[10] L. Zaitseva, R. Myers, A. Fassati, TRNAs promote nuclear import of HIV-1 intracellular reverse transcription complexes, PLoS Biol. 4 (2006) e332.
[11] M. Bukrinsky, A. Adzhubei, Viral protein R of HIV-1, Rev. Med. Virol. 9 (1999) 39–49.
[12] Y. Nitahara-Kasahara, M. Kamata, T. Yamamoto, X. Zhang, Y. Miyamoto, K. Muneta, S. Iijima, Y. Yoneda, Y. Tsunetsugu-Yokota, Y. Aida, Novel nuclear import of Vpr promoted by Importin α is crucial for human immunodeficiency virus type 1 replication in macrophages, J. Virol. 81 (2007) 5284–5293.
[13] M. Bouyac-Bertoia, J.D. Dvorin, R.A. Fouchier, Y. Jenkins, B.E. Meyer, L.I. Wu, M. Emerman, M.H. Malim, HIV-1 infection requires a functional integrase NLS, Mol. Cell 7 (2001) 1025–1035.
[14] M. Kamata, Y. Nitahara-Kasahara, Y. Miyamoto, Y. Yoneda, Y. Aida, Importin-α promotes passage through the nuclear pore complex of human immunodeficiency virus type 1 Vpr, J. Virol. 79 (2005) 3557–3564.
[15] O.J. Cohen, A.S. Fauci, Current strategies in the treatment of HIV infection, Adv. Intern. Med. 46 (2001) 207–246.
[16] X. Wen, K.M. Duus, T.D. Friedrich, C.M. de Noronha, The HIV1 protein Vpr acts to promote G2 cell cycle arrest by engaging a DDB1 and Cullin4A-containing ubiquitin ligase complex using VprBP/DCAF1 as an adaptor, J. Biol. Chem. 282 (2007) 27046–27057.
[17] A. Azuma, A. Matsuo, T. Suzuki, T. Kurosawa, X. Zhang, Y. Aida, Human immunodeficiency virus type 1 Vpr induces cell cycle arrest at the G(1) phase and apoptosis via disruption of mitochondrial function in rodent cells, Microbes Infect. 8 (2006) 670–679.
[18] M. Kuramitsu, C. Hashizume, N. Yamamoto, A. Azuma, M. Kamata, Y. Tanaka, Y. Aida, A novel role for Vpr of human immunodeficiency virus type 1 as a regulator of the splicing of cellular pre-mRNA, Microbes Infect. 7 (2005) 1150–1160.
[19] C. Hashizume, M. Kuramitsu, X. Zhang, T. Kurosawa, M. Kamata, Y. Aida, Human immunodeficiency virus type 1 Vpr interacts with spliceosomal protein SAP145 to mediate cellular pre-mRNA splicing inhibition, Microbes Infect. 9 (2007) 490–497.
[20] N. Yamamoto, C. Tanaka, Y. Wu, M.O. Chang, Y. Inagaki, Y. Saito, T. Naito, H. Ogasawara, I. Sekigawa, Y. Hayashida, Analysis of human immunodeficiency virus type 1 integration by using a specific, sensitive and quantitative assay based on real-time polymerase chain reaction, Virus Genes 32 (2006) 105–113.
[21] S. Mahalingam, V. Ayyavoo, M. Patel, T. Kieber-Emmons, D.B. Weiner, Nuclear import, virion incorporation, and cell cycle arrest/differentiation are mediated by distinct functional domains of human immunodeficiency virus type 1 Vpr, J. Virol. 71 (1997) 6339–6347.
[22] B. Bowerman, P.O. Brown, J.M. Bishop, H.E. Varmus, A nucleo-protein complex mediates the integration of retroviral DNA, Genes Dev. 3 (1989) 469–478.

Immunology Letters 123 (2009) 149–154

Contents lists available at ScienceDirect

Immunology Letters

journal homepage: www.elsevier.com/locate/

Immune impairment thresholds in HIV infection

Shingo Iwami[a], Shinji Nakaoka[b,c], Yasuhiro Takeuchi[a,*], Yoshiharu Miura[d,e], Tomoyuki Miura[f]

[a] Graduate School of Science and Technology, Shizuoka University, 3-5-1 Johoku Naka-ku, Hamamatsu 432-8561, Japan
[b] Aihara Complexity Modelling Project, ERATO, JST, The University of Tokyo, Japan
[c] Graduate School of Mathematical Sciences, The University of Tokyo, Japan
[d] Laboratory of Viral Pathogenesis, Institute for Virus Research, Kyoto University, Japan
[e] Department of Neurology, Saitama Prefectural Rehabilitation Center, Japan
[f] Laboratory of Primate Model, Institute for Virus Research, Kyoto University, Japan

ARTICLE INFO

Article history:
Received 1 December 2008
Received in revised form 10 March 2009
Accepted 10 March 2009
Available online 24 March 2009

Keywords:
HIV infection
Dendritic cell
Immune impairment
Immunodeficiency
Distribution of asymptomatic period
Mathematical model

ABSTRACT

Longitudinal studies of patients infected with HIV-1 reveal a long and variable length of asymptomatic phase between infection and development of AIDS. Some HIV infected patients are still asymptomatic after 15 or more years of infection but some patients develop AIDS within 2 years. The mechanistic basis of the disease progression has remained obscure but many researchers have been trying to explain it. For example, the possible importance of viral diversity for the disease progression and the development of AIDS has been very well worked out in the early-1990s, especially by some important works of *Martin A. Nowak*. These studies can give an elegant explanation for a variability of asymptomatic phase. Here, a simple mathematical model was used to propose a new explanation for a variable length of asymptomatic phase. The main idea is that the immune impairment rate increases over the HIV infection. Our model suggested the existence of so-called "Risky threshold" and "Immunodeficiency threshold" on the impairment rate. The former implies that immune system *may* collapse when the impairment rate of HIV exceeds the threshold value. The latter implies that immune system *always* collapses when the impairment rate exceeds the value. We found that the length of asymptomatic phase is determined stochastically between these threshold values depending on the virological and immunological states. Furthermore, we investigated a distribution of the length of asymptomatic phase and a survival rate of the immune responses in one HIV patient.

1. Introduction

The infection with HIV-1 is characterized by various patterns of the disease progression among the patients [18,49]. Longitudinal studies of the patients reveal a long and variable length of latency (asymptomatic) phase between infection and development of AIDS [3,13,28,45]. Some HIV infected patients are still asymptomatic after 15 or more years of infection but some patients develop AIDS within 2 years [4,27](the similar disease progression patterns are also observed in SIV/SHIV infected individuals [2,21]). Although the mechanistic basis of the disease progression has remained obscure, several factors such as viral reproductive abilities and immune proliferative abilities are considered as a cause of the diverse disease progression [1,10,11,14,15,19,29,47].

Above all, the possible importance of viral diversity for the disease progression and the development of AIDS have been very well worked out in the early-1990s, especially by some important works of *Martin A. Nowak* [29–33]. These very interesting studies revealed the potential existence of viral diversity threshold which states that the viral load explodes when the diversity of virus strains exceeds this threshold number. Although the diversity threshold theory can give an elegant explanation for variability of asymptomatic phase, there are several unverificational and skeptical points over HIV/SIV/SHIV disease progression (for example, the difficulty of detection of the number of quasispecies, the disease progression without increasing the viral diversity, and the limitation of viral diversity are included), and therefore it might be difficult to validate this theory by experiments.

Here we construct a simple mathematical model describing the interactions between HIV and immune cells and propose a new explanation for the variable length of asymptomatic phase in HIV infection. The main idea is that immune impairment effect increases over the HIV infection. This idea is naturally justified by progressive decrease of dendritic cell (DC) number and function, which are crucial in generation and regulation of adaptive immunity such as cytotoxic T lymphocytes (CTLs), during the course of HIV infection [8,9,23,42,43,48].

Our model suggests the existence of two thresholds: one is "Risky threshold" which states that immune system may collapse

* Corresponding author. Tel.: +81 53 478 1200; fax: +81 53 478 1200.
E-mail address: takeuchi@sys.eng.shizuoka.ac.jp (Y. Takeuchi).

0165-2478/$ – see front matter © 2009 Elsevier B.V. All rights reserved.
doi:10.1016/j.imlet.2009.03.007

when the impairment rate of HIV exceeds the threshold value (a risk of immunodeficiency) and the other is "Immunodeficiency threshold" which states that immune system always collapses when the impairment rate exceeds the value (a fatality of immunodeficiency). We found that the length of asymptomatic phase is determined stochastically between these threshold values depending on the virological and immunological states. Furthermore, we investigated a distribution of the length of asymptomatic phase and a survival rate of the immune responses in one HIV patient.

2. Methods

After encountering HIV in the peripheral blood, DCs mature and travel to lymphoid organs [8,18]. The matured DCs present HIV on MHC class II to prime $CD4^+$T cells to become activated $CD4^+$T cells which can secrete helper signals (e.g. IL-2) [14,18]. Furthermore, the DCs cross-present HIV on MHC class I to prime $CD8^+$T cells. By receiving antigen signal from the DCs and helper signal from activated $CD4^+$T cells, $CD8^+$ T cells expand and differentiate into CTLs to kill HIV infected cells [18,26,41,49]. Here we use a simple mathematical model describing the interactions between HIV and immune cells and explain about our modeling approach, basic assumptions, and scenario in detail.

2.1. Dynamics of HIV replication and CTL inducement

As described in [5,44], we only consider activated $CD4^+$T cells (x) as target cells for HIV. This is because other cell populations bearing CD4 molecule such as naive $CD4^+$T cells, resting $CD4^+$ T cells and macrophages are less commonly infected by HIV compared with activated $CD4^+$ T cells [5,14,44]. We assume that activated $CD4^+$T cells are produced at a rate of λ cells day^{-1}, decay at a rate d day^{-1}[5,44], and can become infected at a rate proportional to the number of infected $CD4^+$T cells (y) with transmission rate constant βday^{-1}cell^{-1}[17,47]. The infected $CD4^+$T cells are assumed to decay at a rate a day^{-1}.

In order to suppress HIV replication, our immune system induces CTL responses through the interactions with DCs. Here we consider that CTL responses (z) include both CTL effector and memory (CTL naives are assumed to be described by initial value of z). The CTL responses eliminate infected $CD4^+$ T cells at a rate proportional to the number of CTLs with killing rate constant p day^{-1}cell^{-1} and decay at a rate b day^{-1}[17,47]. We simply assume that proliferation of CTLs (i.e., expansion and differentiation) requires both antigen and helper signal [18,26,41,49] and its rate is c day^{-1}cell^{-2}. This implies that, in the absence of any immune impairment effects, the proliferation is described by $cxyz$ [1,36,47]. However, in the presence of immune impairment effects caused by HIV infection, CTL proliferation is reduced (we give a detailed explanation in later). Therefore, we model immune impairment effects as $cxyz/(1+\varepsilon y)$. Here we mention that the impairment effect depends on the number of infected $CD4^+$T cells and ε represents immune impairment rate.

2.2. Mathematical model

We extend the standard virus-immune model [29] including the effect of immune impairment caused by HIV infection. Our mathematical model is given by the following equation:

$$x' = \lambda - dx - \beta xy, \quad y' = \beta xy - ay - pyz, \quad z' = \frac{cxyz}{1+\varepsilon y} - bz \quad (1)$$

Because free virus populations decay at much faster rates than the other T cells, we can assume that the virus population is in a quasi steady state [46], and the dynamics of free virus is neglected in model (1)[17,47].

2.3. Immune impairment effect over HIV infection

Several DC populations are targets for HIV [14,22,48] and, as a consequence, the ability of DCs (e.g. antigen presentation) to stimulate T cell proliferation is impaired because of depletion and dysfunction of DC (e.g. downregulation of CD80/86 and MHC II expression) [8,9,20,22,23,35]. The evidence comes from observations that DCs express CD4 and chemokine receptors and are susceptible to HIV infection in vitro [35,48]. Actually, progressive depletion of DC and its functional defects, which would in turn impair generation of CTLs, in patients with HIV-1 infection are observed [8,9,23] and the reduction of DC number and function is particularly marked in patients with AIDS compared with asymptomatic subjects [23,35]. Therefore, the progressive change of DC might contribute to the immunodeficiency associated with HIV-1 disease [8,9,20,22,23,35,48]. In order to understand how the progressive depletion and functional defect of DCs affect disease symptoms, we simply assume that the immune impairment rate (ε) gradually increases and therefore CTL proliferation decreases over the HIV infection.

2.4. Pathological scenario

Usually, after infection of HIV, the virus establishes the acute infection [29]. This implies that basic reproduction number of the virus, $R_0 = \lambda\beta/ad$, is greater than 1. Furthermore, at the end of the acute infection, CTL responses are induced and the infected cells are regulated by them at a virological set point [18,26]. That is, most of patients progress to asymptomatic phase which follows the acute phase and remain at this phase for a long time, which represents a typical disease progression of HIV infection.

Actually, if the viral infectivity (i.e., infection rate of HIV: β) is remarkably large, in the sense that $\lambda c/b < \beta$, our immune system do not establish CTL responses in spite of very high viral load. Because too much $CD4^+$T cells are destroyed during the acute infection, infected individuals immediately develop immunodeficiency without the asymptomatic phase, which represents a rapid disease progression observed in experimental SIV/SHIV infection [2,21].

On the other hand, if the cytopathogenicity is not small, in the sense that $\lambda\beta/d - \beta\sqrt{\lambda cb\beta}/cd < a$, CTL responses are hardly or not observed because of lack of antigen signals. These phenomena are considered as CTL non-responsiveness which is different from immunodeficiency of HIV infection [47](AIDS is characterized by high virus load of HIV and $CD4^+$ T cell depletion [18]). The CTL non-responsiveness might be observed in a viral infection with a high degree of cytopathogenicity but can not be applied to HIV infection.

Therefore, because we focus on the typical HIV disease progression in this paper, we assume that:

$$1 < R_0, \quad \beta < \frac{\lambda c}{b}, \quad 0 < a < \frac{\lambda\beta}{d} - \frac{\beta\sqrt{\lambda cb\beta}}{cd}$$

The detailed mathematical explanation for the derivation of the above thresholds is given in [16].

3. Results

We investigate how loss of DC number and function (i.e., increase of immune impairment rate) correlates with the development of immunodeficiency and discuss with a distribution of the length of asymptomatic phase.

3.1. Risky and immunodeficiency thresholds

We demonstrate the existence of immune impairment thresholds which can determine patients' symptoms.

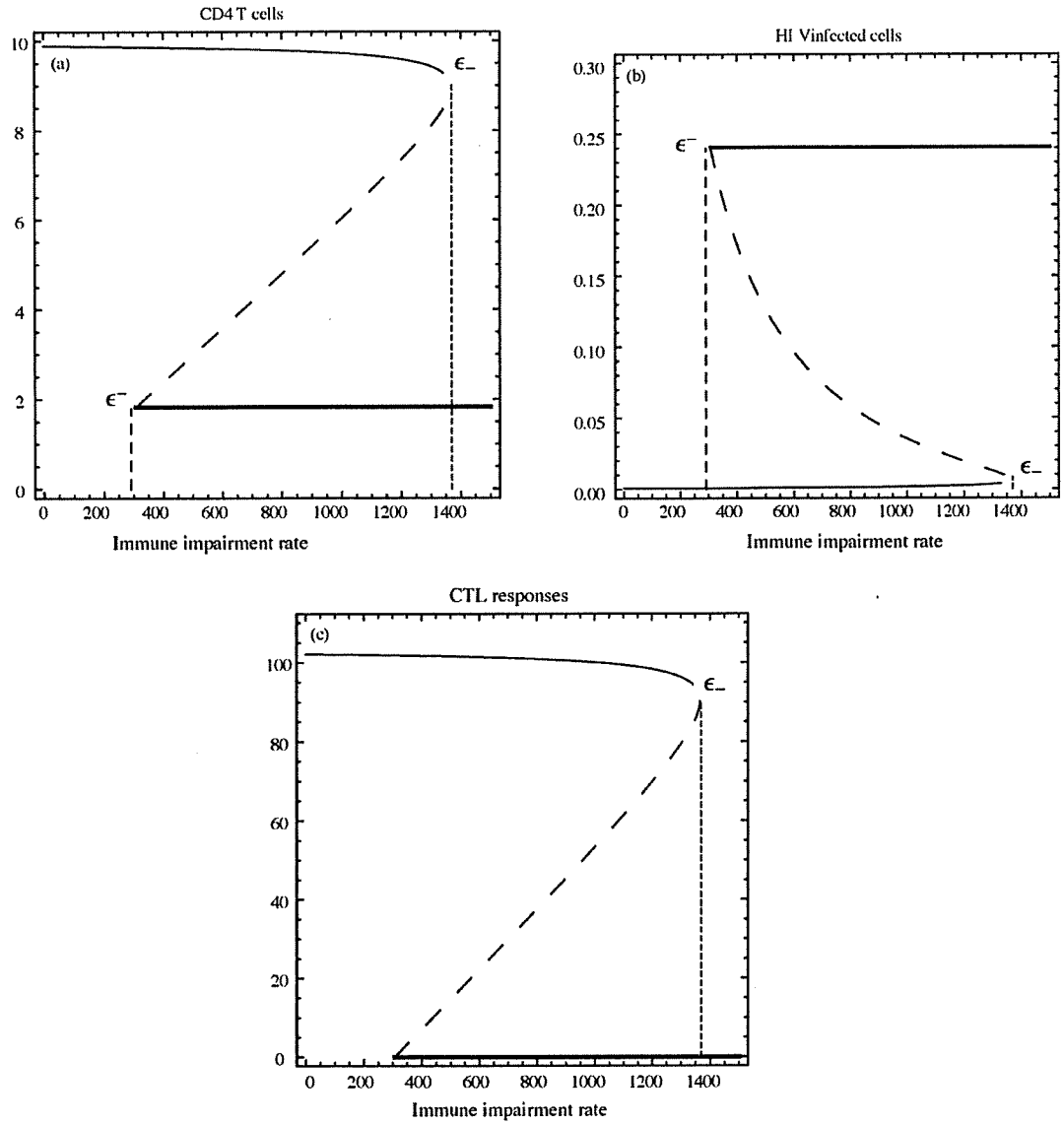

Fig. 1. Typical disease progression in HIV infection: the black and red solid lines, respectively, represent each cell number at the controlled and immunodeficiency state over HIV infection (the black dashed lines represent each cell number at E_c^-). Because the immune impairment rate is small at the beginning of the infection, the sustained CTLs suppress HIV replication. However, the CTL responses gradually decrease and the infected individuals become to have a risk of development of AIDS, if the impairment rate exceeds the risky threshold (i.e., $\tilde{\varepsilon} < \varepsilon$), and they always develop AIDS, if the rate exceeds the immunodeficiency threshold (i.e., $\varepsilon_- < \varepsilon$). Here we choose our baseline parameter values as follows: $\lambda = 0.1089$, $d = 0.01089$, $\beta = 0.2027$, $a = 0.366$, $p = 0.016$, $c = 2.13$, and $b = 0.0125$. These values are based on previously estimated parameter values in [7,24,34,44]. Because we are interested in change of immune impairment effect and their threshold phenomena, we set ε a free parameter. The detailed explanation of the estimate of our baseline parameter values is given in [16]. (For interpretation of the references to color in this figure legend, the reader is referred to the web version of the article.)

Because we assumed a relatively small infection rate (β) and cytopathogenicity of HIV (a), sustained CTL responses are established and therefore the viral replication is suppressed at a low level in "controlled state" $E_c^+ = (x_c^+, y_c^+, z_c^+)$ after the acute infection. Actually our model has another possible interior equilibrium $E_c^- = (x_c^-, y_c^-, z_c^-)$ but E_c^- is not biologically appropriate because the equilibrium is always unstable even if it exists [16].

However, as immune impairment rate increases, the CTL responses gradually become weak and the infected individuals eventually develop immunodeficiency (i.e., AIDS) because of depletion of CD4$^+$T cells (Fig. 1). This progressive immune decline corresponds to the typical disease progression of HIV infection [18]. Over the disease progression, we have the following two immune impairment thresholds which can characterize the development of AIDS:

$$\tilde{\varepsilon} = \frac{ac}{b\beta} + \frac{a\beta}{ad - \lambda\beta}, \qquad \varepsilon_- = \frac{\left(\sqrt{b\beta} - \sqrt{\lambda c}\right)^2}{bd}$$

Until the impairment rate exceeds $\tilde{\varepsilon}$, CTLs control the virus load at very low level, but if the impairment rate exceeds this threshold value, the patient has a risk of development of AIDS (Fig. 1). This is because, in this case, "immunodeficiency state" $E_u = (x_u, y_u, 0)$ is stable, in which a complete breakdown of our immune system occurs (i.e., z converges to 0), and both the controlled and immunodeficiency states can be stable simultaneously. Here we call $\tilde{\varepsilon}$ "Risky threshold".

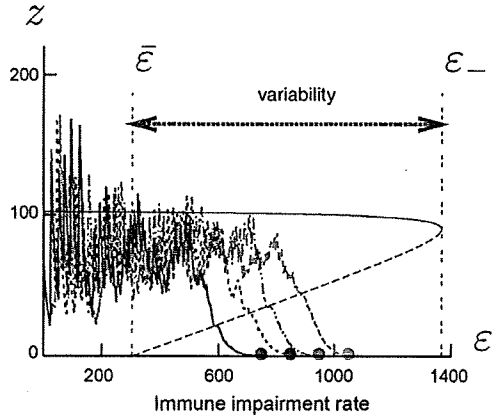

Fig. 2. Development of AIDS caused by stochastic perturbations: we calculate time-course of the disease progression in the context of stochastic perturbations. The stochastic perturbations can occur in the CTL proliferation $cxyz/(1+\varepsilon y+\xi)$, where ξ is a noise measured by a lognormal distribution. We assume that, because of progressive depletion and dysfunction of DC, the immune impairment accumulates with a very low rate during disease progression, $\varepsilon(t) = 0.25t$, where 0.25 is the rate of average impairment per day. The most severe patient (red line) develops AIDS after the impairment rate exceeds around 700. However, the most mild patient (green line) do not develop AIDS until the rate exceeds around 1000. The development of AIDS is determined stochastically between these threshold values depending on the virological and immunological states. Therefore, we can explain the variable length of asymptomatic phase in HIV infection. Here we use the same parameter values in Fig. 1. The risky and immunodeficiency thresholds, respectively, are estimated to $\bar{\varepsilon} = 303.63$ and $\varepsilon_- = 1366.45$. (For interpretation of the references to color in this figure legend, the reader is referred to the web version of the article.)

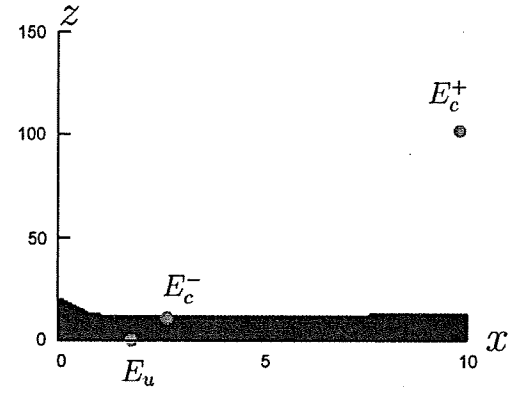

Fig. 3. Risky zone of immunodeficiency: we plot a basin of attraction of E_u as red region and call it "Risky zone". Until the immune impairment rate (ε) exceeds the risky threshold ($\bar{\varepsilon}$), only E_c^+ is stable. On the other hand, when the impairment rate exceeds the risky threshold, E_c^- is generated into $\mathbb{R}^3_+$ via a transcritical bifurcation with E_u and the risky zone emerges (i.e, both E_c^+ and E_u become stable simultaneously). The stable manifold of E_c^- forms boundary surface of the risky zone. And also, the risky zone expands during the impairment rate increases until the immunodeficiency threshold (ε_-). However, once the impairment rate exceeds the immunodeficiency threshold, $E_c^\pm$ are degenerated via a saddle-node bifurcation and full space becomes the risky zone (i.e, only E_u is stable). Here we use the same parameter values in Fig. 1 and set $\varepsilon = 450$.

Furthermore, once the impairment rate exceeds ε_-, our immune system completely collapses, CTL responses become inactivated and the patient always develops AIDS (Fig. 1). This is because the controlled equilibrium is degenerated but the immunodeficiency equilibrium remains stable. We call ε_-"Immunodeficiency threshold".

3.2. Development of AIDS

The development of AIDS in the patient might be affected by stochastic perturbations caused by virological and immunological events, such as mutational changes of viral epitopes and their specific immune responses [25,26,29], a switch of coreceptor from CCR5 to CXCR4 [18,37], and an emergence of drug resistance [38]. Here we investigate an impact of the stochastic perturbations on a deterioration of the disease (Fig. 2).

Usually, virus load of HIV equilibrates and remains at a virological set point just after the acute infection [18,26]. Even if the immune impairment rate increases, the viral replication is well controlled by CTL responses at the controlled state until the rate exceeds the risky threshold (i.e., $0 < \varepsilon < \bar{\varepsilon}$). This is because only E_c^+ is stable, and therefore the immune suppression is robust for any stochastic perturbation (Fig. 2).

However, when the impairment rate exceeds the risky threshold (i.e., $\bar{\varepsilon} < \varepsilon$), the stochastic perturbations lead to the development of immunodeficiency (Fig. 2) because of the bistability of controlled state and immunodeficiency state. Furthermore, to investigate a progressive risk of immunodeficiency, we plot a basin of attraction (i.e., absorbing region) of E_u as red region which is called "Risky zone" in Fig. 3 (if their virological and immunological states are located on the risky zone, an HIV patient eventually develops immunodeficiency). Because the risky zone gradually expands during the impairment rate increases (simulations are not shown) until the immunodeficiency threshold ($\varepsilon < \varepsilon_-$), the patient becomes sensitive to these stochastic perturbations (i.e., the risk of the development of immunodeficiency is progressively increased).

In addition, once the impairment rate exceeds the immunodeficiency threshold ($\varepsilon_- < \varepsilon$), the risky zone expands into total space (simulations are not shown) and the patient always develops AIDS because the immunodeficiency state E_u becomes unique stable steady state.

Thus, the development of AIDS (i.e., the length of asymptomatic phase) is determined stochastically between these threshold values depending on the virological and immunological states (Fig. 2).

3.3. Distribution of length of asymptomatic phase

It is a well-known empirical fact that incubation times of most diseases obey a lognormal distribution that is often referred to as 'Sartwel's model' [19,40]. For example, the waiting times between HIV infection and the development of AIDS is considered as a lognormal distribution. We mention that these results are based on cross-sectionally epidemiological studies of the HIV patients from around the world [3,13,45]. Actually, it is poorly understood how the incubation times (i.e., the possibility of the development of AIDS) are distributed in one HIV patient. Here we study the distribution of the length of asymptomatic phase (i.e., a probability density function of development of AIDS) based on within host dynamics (1) in one HIV patient which shows the typical disease progression.

We calculate 1000 trials of time-course of the disease progression in the context of stochastic perturbations and investigate frequency of the development of immunodeficiency at each immune impairment rate in Fig. 4. The histogram in Fig. 4 represents a distribution of the length of asymptomatic phase (the median values $\varepsilon = 986.61$). Here we simply assume that the length of asymptomatic phase is represented by the immune impairment rate at which CTL responses vanish. The blue curve drawn by solid line in Fig. 4 represents a survival rate of the immune responses (i.e., the probability that an HIV patient has not yet developed AIDS at each impairment rate). The two dashed-curves represent a 95% confidence interval of the survival rate.

Because the patient does not develop AIDS until the impairment rate exceeds the risky threshold, the distribution (or the median value) leans to the range of large impairment rate and the survival

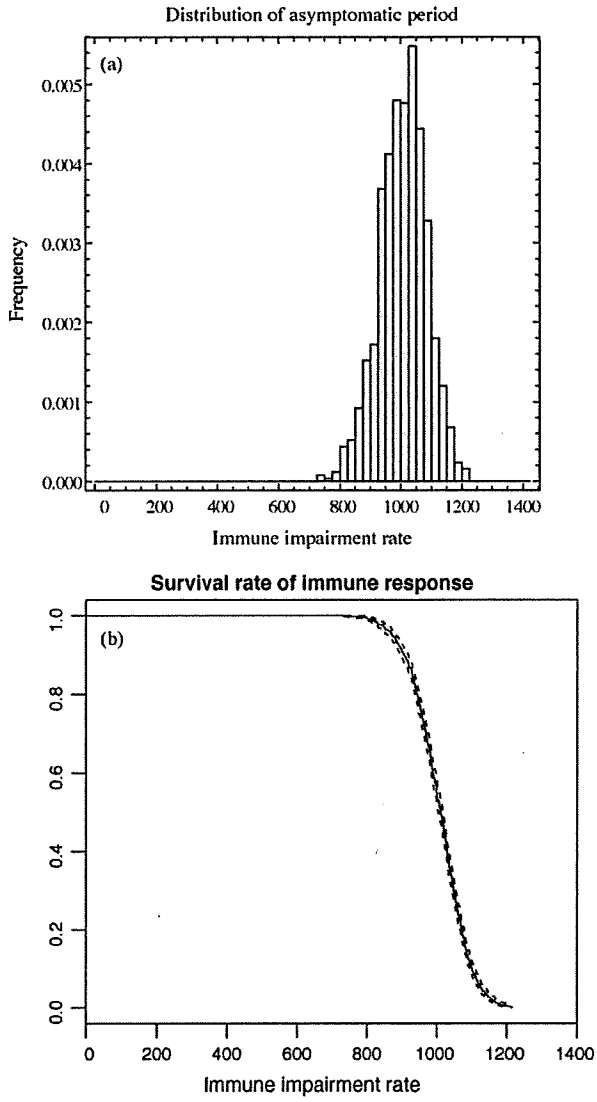

Fig. 4. Distribution of length of asymptomatic phase: we calculate 1000 trials of time-course of the disease progression in the context of stochastic perturbations (we use the same method in Fig. 2) and investigate frequency of the development of immunodeficiency at each immune impairment rate. The left histogram represents a distribution of the length of asymptomatic phase (here we simply consider that the length of asymptomatic phase is represented by the immune impairment rate at which CTL responses vanish). We assume that the categories of the histogram are 60 and the scale of the histogram is 1 (i.e., each category represents a probability density). The right function drawn by solid blue line represents a survival rate of the immune responses (i.e., the probability that an HIV patient has not yet developed AIDS at each impairment rate). The two dashed-lines represent a 95% confidence interval of the survival rate. Estimation for the distribution of the survival rate is computed with GNU R package for survival analysis. These results imply the existence of long and variable asymptomatic phase between infection and development of AIDS. Here we use the same parameter values in Fig. 1. The risky and immunodeficiency thresholds, respectively, are estimated to $\bar{\varepsilon} = 303.63$ and $\varepsilon_{-} = 1366.45$. (For interpretation of the references to color in this figure legend, the reader is referred to the web version of the article.)

curve is flat in the range of small impairment rate. However, because the patient has a (stochastic) risk of development of AIDS once the rate exceeds the risky threshold and the risk is progressively increased until the immunodeficiency threshold, the distribution tends to have a center peak and the survival curve begins to decay gradually. Furthermore, because the patient always develops AIDS after the impairment rate exceeds the second threshold, the shape of the distribution is characterized by a short right tail and the survival rate vanishes.

Thus, we obtain the relatively wide shape of the distribution of the length of asymptomatic phase between the risky thresholds and immunodeficiency thresholds and a gradually decreasing function of the survival rate of the immune responses. These results predict the existence of long and variable asymptomatic phase between infection and development of AIDS.

4. Discussion

The origin of various disease progression in HIV infection is largely unresolved but many researchers have been trying to explain it. An important factor in understanding the unusual incubation period distribution in the development of AIDS is the dynamics of the long-lasting struggle between HIV and our immune system [19]. Until now, several approaches have been proposed to explain the long-term fight in HIV infection [1,10,11,14,15,19,29,47]. For example, in very early models of HIV infection worked by *Martin A. Nowak*, increasing of HIV variants' diversity, which leads to an explosion in the virus load, explained the collapse of immune system after a long incubation period. They claimed the possible importance of viral diversity for the disease progression and the development of AIDS [29–33].

Here we discussed about an immune impairment effect caused by the depletion and dysfunction of DC on HIV disease progression. Because the progressive decrease of DC number and function during the course of HIV-1 infection is observed [8,9,23], we simply assumed that the immune impairment rate (ε) increases over the HIV infection instead of directly considering a population dynamics of DCs. In the typical disease progression which is characterized by relatively small infection rate (β) and cytopathogenicity of HIV (a), we demonstrated that increasing of immune impairment rate eventually leads to the development of immunodeficiency and proposed the possibility of the existence of the risky threshold ($\bar{\varepsilon}$) and the immunodeficiency threshold (ε_{-}) over the disease progression (Figs. 1 and 2). Our theoretical framework can explain the disease progression as many experimenters hypothesized that the progressive alteration of the immune system (the depletion and dysfunction of DCs are central to many of these hypotheses) might be caused by the development of AIDS [8,9,20,22,23,35,42,48].

Using our within host dynamics model (1), we also investigated a distribution of the length of asymptomatic phase for a typical disease progressor in Fig. 4. From cross-sectionally epidemiological studies of the HIV patients from around the world, it is said that the distribution among the patients is considered as a lognormal distribution [3,13,45](e.g. a cellular automaton model with a sequence space framework reported that the incubation time is a lognormal-like distribution [19]). However, our predictable distribution based on the within host dynamics in one HIV patient is different from the well-known distribution obtained by the cross-sectional studies (actually, it is difficult to reveal the distribution in one HIV patient from epidemiological data). The shape of the distribution is characterized by the center peak and the short right tail. Furthermore, the right tail of the distribution might be characterized by a small peak at the end, if stochastically long-term-survival trials exist (simulations are not shown), because the patient always develops AIDS above the immunodeficiency threshold. Thus, our theoretical framework leads to an epidemiologically-falsifiable (or -difficult) predictions which merit further experimental investigations in SIV/SHIV infection.

In summary, we found that increasing of the immune impairment rate caused by the progressive decrease of DC number and function plays an important role in HIV infection. This implies that

recovering DC function and increasing DC number are effective in inducing immune response and delaying the disease progression (actually, several studies of DC immunotherapy found transient decrease of the virus load by activating T cell responses against HIV-1 [6,12,39]) because the modulation of DC leads to decrease of the immune impairment rate. Furthermore, if the impairment rate can be quantified by time-course data of DCs [8,9,23], our theory might enable to predict a real-time risk of the development of AIDS for each patients.

Conflict of interest

The authors have no competing interests.

Acknowledgments

We would like to thank anonymous referees and the editor for very helpful suggestions and comments which improved the quality of this paper and study.

SI was supported by Research Fellowships of the Japan Society for the Promotion of Science for Young Scientists and SN was supported by (i) Research Fellowships of the Japan Society for the Promotion of Science for Young Scientists and (ii) the Sasakawa Scientific Research Grant from The Japan Science Society.

Author contributions: All authors conceived the model and analyzed the model. SI wrote the paper.

References

[1] Altes HK, Wodarz D, Jansen VAA. The dual role of CD4 T helper cells in the infection dynamics of HIV and their importance for vaccination. J Theor Biol 2002;214:633–46.
[2] Binley JM, Clas B, Gettie A, Vesanen M, Montefiori DC, Sawyer L. Passive infusion of immune serum into simian immunodeficiency virus-infected rhesus macaques undergoing a rapid disease course has minimal effect on plasma viremia. Virology 2000;270:237–49.
[3] CASCADE Collaboration. Time from HIV-1 seroconversion to AIDS and death before widespread use of highlyactive antiretroviral therapy: a collaborative re-analysis. Lancet 2000; 355:1131–7.
[4] Cecilia D, Kleeberger C, Munoz A, Giorgi JV, Zolla-Pazner S. A longitudinal study of neutralizing antibodies and disease progression in HIV-1-infected subjects. J Infect Dis 1999;179:1365–74.
[5] Ciupe MS, Bivort BL, Bortz DM, Nelson PW. Estimating kinetic parameters from HIV primary infection data through the eyes of three different mathematical models. Math Biosci 2006;200:1–27.
[6] Connolly NC, Whiteside TL, Wilson C, Kondragunta V, Rinaldo CR, Riddler SA. Therapeutic immunization with human immunodeficiency virus type 1 (HIV-1) peptide-loaded dendritic cells is safe and induces immunogenicity in HIV-1-infected individuals. Clin Vaccine Immunol 2008;15:284–92.
[7] Davenport MP, Ribeiro RM, Perelson AS. Kinetics of virus-specific CD8+ T cells and the control of human immunodeficiency virus infection. J Virol 2004;78:10096–103.
[8] Donaghy H, Pozniak A, Gazzard B, Qazi N, Gilmour J, Gotch F. Loss of blood CD11c+ myeloid and CD11c- plasmacytoid dendritic cells in patients with HIV-1 infection correlates with HIV-1 RNA virus load. Blood 2001;98:2574–6.
[9] Donaghy H, Gazzard B, Gotch F, Patterson S. Dysfunction and infection of freshly isolated blood myeloid and plasmacytoid dendritic cells in patients infected with HIV-1. Blood 2003;101:4505–11.
[10] de Boer RJ, Boerlijst MC. Diversity and virulence thresholds in AIDS. Proc Natl Acad Sci USA 1994;94:544–8.
[11] Galvani AP. The role of mutation accumulation in HIV progression. Proc Roy Soc Lond B 2005;272:1851–8.
[12] Garcia F, Lejeune M, Climent N, Gil C, Alcami J, Morente V. Therapeutic immunization with dendritic cells loaded with heat-inactivated autologous HIV-1 in patients with chronic HIV-1 infection. J Infect Dis 2005;191:1680–5.
[13] Gayet-Ageron A, Baratin D, Marceillac E, Allard R, Peyramond D, Chidiac C. The AIDS epidemic in Lyon: patient characteristics and defining illnesses between 1985 and 2000. HIV Med 2004;5:163–70.
[14] Hogue IB, Bajaria SH, Fallert BA, Qin S, Reinhart TA, Kirschner DE. The dual role of dendritic cells in the immune response to human immunodeficiency virus type 1 infection. J Gen Virol 2008;89:2228–39.
[15] Iwami S, Nakaoka S, Takeuchi Y. Viral diversity limits immune diversity in asymptomatic phase of HIV infection. Theor Pop Biol 2008;73:332–41.
[16] Iwami S, Miura T, Nakaoka S, Takeuchi Y. Immune impairment effect in HIV infection: existence of risky and immunodeficiency thresholds. J Theor Biol, in press.
[17] Iwasa Y, Michor F, Nowak MA. Virus evolution within patients increases pathogenicity. J Theor Biol 2005;232:17–26.
[18] Janewa C, Travers P, Walport M, Shlomchik MJ. Immunobiology: the immune system in health and disease. Garland Pub.; 2004.
[19] Kamp C, Bornholdt S. From HIV infection to AIDS: a dynamically induced percolation transition? Proc Roy Soc Lond B 2002;269:2035–40.
[20] Kawamura T, Gatanaga H, Borris DL, Connors M, Mitsuya H, Blauvelt A. Decreased stimulation of CD4+ T cell proliferation and IL-2 production by highly enriched populations of HIV-infected dendritic cells. J Immunol 2003;170:4260–6.
[21] Kozyrev IL, Ibuki K, Shimada T, Kuwata T, Takemura T, Hayami M. Characterization of less pathogenic infectious molecular clones derived from acute-pathogenic SHIV-89.6P stock virus. Virology 2001;282:6–13.
[22] Lore K, Sonnerborga A, Brostrom C, Goh L-E, Perrin L, McDade H. Accumulation of DC-SIGN+CD40+ dendritic cells with reduced CD80 and CD86 expression in lymphoid tissue during acute HIV-1 infection. AIDS 2002;16:683–92.
[23] Macatonia SE, Lau R, Patterson S, Pinching AJ, Knight SC. Dendritic cell infection, depletion and dysfunction in HIV-infected individuals. Immunology 1990;71:38–45.
[24] Mandl JN, Regoes RR, Garber DA, Feinberg MB. Estimating the effectiveness of simian immunodeficiency virus-specific CD8+ T cells from the dynamics of viral immune escape. J Virol 2007;81:11982–91.
[25] McKnight A, Clapham PR. Immune escape and tropism of HIV. Tre Micro 1995;3:356–61.
[26] McMichael AJ, Rowland-Jones SL. Cellular immune responses to HIV. Nature 2001;410:980–7.
[27] Meissnera EG, Duus KM, Gao F, Yu X-F, Su L. Characterization of a thymustropic HIV-1 isolate from a rapid progressor: role of the envelope. Virology 2004;328:74–88.
[28] Mellors JW. Viral-load tests provide valuable answers. Sci Am 1998. July:70.
[29] Nowak MA, May RM. Virus dynamics. Oxford University Press; 2000.
[30] Nowak MA. Evolutionary dynamics. Harvard University Press; 2006.
[31] Nowak MA, Anderson RM, McLean AR, Wolfs TF, Goudsmit J, May RM. Antigen diversity thresholds and the development of AIDS. Science 1991;15:963–9.
[32] Nowak MA. Variability in HIV infections. J Theor Biol 1992;155:1–20.
[33] Nowak MA, May RM. AIDS pathogenesis: mathematical models of HIV and SIV infection. AIDS 1993;7:S3–18.
[34] Ogg GS, Jin X, Bonhoeffer S, Moss P, Nowak MA, Monard S. Decay kinetics of human immunodeficiency virus-specific effector cytotoxic T lymphocytes after combination antiretroviral therapy. J Virol 1999;73:797–800.
[35] Patterson S, English NR, Longhurst H, Balfe P, Helbert M, Pinching AJ. Analysis of human immunodeficiency virus type 1 (HIV-1) variants and levels of infection in dendritic and T cells from symptomatic HIV-1-infected patients. J Gen Virol 1998;79:247–57.
[36] Regoes RR, Wodarz D, Nowak MA. Virus dynamics: the effect of target cell limitation and immune responses on virus evolution. J Theor Biol 1998;191:451–62.
[37] Regoes RR, Bonhoeffer S. The HIV coreceptor switch: a population dynamical perspective. Tre Micro 2005;13:269–77.
[38] Richman DD. HIV chemotherapy. Nature 2001;410:995–1001.
[39] Rinaldo CR. Dendritic cell-based human immunodeficiency virus vaccine. J Int Med 2008;265:138–58.
[40] Sartwell P. The incubation period and the dynamics of infectious disease. Am J Epidemiol 1966;83:204–16.
[41] Schmitz JE, Kuroda MJ, Santra S, Sasseville VG, Simon MA, Lifton MA. Control of viremia in simian immunodeficiency virus infection by CD8(+) lymphocytes. Science 1999;283:857–60.
[42] Smed-Sorensen A, Lore K, Walther-Jallow L, Anderson J, Spetz A. HIV-1 infected dendritic cells up-regulate cell surface markers but fail to produce IL-12 p70 in response to CD40 ligand stimulation. Blood 2004;104:2810–7.
[43] Soumelis V, Scott I, Gheyas F, Bouhour D, Cozon G, Cotte L. Depletion of circulating natural type 1 interferon-producing cells in HIV-infected AIDS patients. Blood 2001;98:906–12.
[44] Stafford MA, Corey L, Cao Y, Daar ES, Ho DD, Perelson AS. Modeling plasma virus concentration during primary HIV infection. J Theor Biol 2000;203:285–301.
[45] Tassie J-M, Grabar S, Lancar R, Deloumeaux J, Bentata M, Costagliola D. Time to AIDS from 1992 to 1999 in HIV-1-infected subjects with known date of infection. J AIDS 2002;30:81–7.
[46] Thieme HR. Mathematics in population biology. Princeton University Press; 2003.
[47] Wodarz D, Klenerman P, Nowak MA. Dynamics of cytotoxic T-lymphocyte exhaustion. Proc Roy Soc Lond B 1998;265:191–203.
[48] Wu L, KewalRamani VN. Dendritic-cell interactions with HIV: infection and viral dissemination. Nat Rev Immunol 2006;6:859–68.
[49] Tunetsugu-Yokota Y. How does HIV infection destory the host immune system? J AIDS Res 2005;7:171–9.

Journal of Theoretical Biology 260 (2009) 490–501

Contents lists available at ScienceDirect

Journal of Theoretical Biology

journal homepage: www.elsevier.com/locate/yjtbi

Immune impairment in HIV infection: Existence of risky and immunodeficiency thresholds

Shingo Iwami [a,*], Tomoyuki Miura [b], Shinji Nakaoka [c,d], Yasuhiro Takeuchi [a]

[a] Graduate School of Science and Technology, Shizuoka University, Japan
[b] Laboratory of Primate Model, Institute for Virus Research, Kyoto University, Japan
[c] Aihara Complexity Modelling Project, ERATO, JST, The University of Tokyo, Japan
[d] Graduate School of Mathematical Sciences, The University of Tokyo, Japan

ARTICLE INFO

Article history:
Received 26 August 2008
Received in revised form
3 June 2009
Accepted 18 June 2009
Available online 3 July 2009

Keywords:
HIV infection
Dendritic cell
Mathematical model
Immune impairment
Immunodeficiency
Bistability
Saddle-node bifurcation
Transcritical bifurcation

ABSTRACT

Results of several studies show that some DC populations are susceptible to HIV. Modulation of DCs by HIV infection, in particular interference of the antigen-presenting function of DCs, is a key aspect in viral pathogenesis and contributes to viral evasion from immunity because the loss of the DC function engenders some impairment effects for a proliferation of CTL responses, which play an important role in the immune response to HIV. As described herein, we use a simple mathematical model to examine virus-immune dynamics over the course of HIV infection in the context of the immune impairment effects. A decrease of the DC number and function during the course of HIV-1 infection is observed. Therefore, we simply assumed that the immune impairment rate increases over the HIV infection. Under the assumption, four processes of the disease progression dynamics of our model are classifiable according to their virological properties. It is particularly interesting a typical disease progression presents a "risky threshold" and an "immunodeficiency threshold". Regarding the former, the immune system *might* collapse when the impairment rate of HIV exceeds a threshold value (which corresponds to a transcritical bifurcation point). For the latter, the immune system *always* collapses when the impairment rate exceeds the value (which corresponds to a saddle-node bifurcation point). To test our theoretical framework, we investigate the existence and distribution of these thresholds in 10 patients.

1. Introduction

A basic principle of immunology has largely been ignored in defining immune parameters of HIV infection: the role of professional antigen presenting cells (APCs)—dendritic cells (DCs), monocytes/macrophages, and B lymphocytes (Rinaldo, 2008). However, these cells play an important role in immune responses (see Fig. 1). In fact, DCs are positioned geographically as sentinels, detecting "danger signals" and linking innate and adaptive immune responses (Donaghy et al., 2001; Rinaldo, 2008). These cells mature and migrate to the secondary lymphoid tissue after they encounter HIV in the periphery (Donaghy et al., 2001; Janewa et al., 2004). The DC maturation process involves increasing antigen presentation on major histocompatibility complex (MHC) molecules, and upregulating co-stimulatory molecules (Hogue et al., 2008; Janewa et al., 2004). The mature DCs present HIV peptides to specific T cells at the lymph nodes and prime antigen-specific $CD4^+$ T cells to become activated $CD4^+$ T cells and $CD8^+$ T cells to differentiate into cytotoxic T lymphocytes (CTLs) (Donaghy et al., 2001; Hogue et al., 2008). Consequently, this cell-based immunity is necessary for fighting HIV infection (Janewa et al., 2004; McMichael and Rowland-Jones, 2001).

However, several studies have revealed that some DC subtypes are susceptible to HIV infection and that the infection engenders interference of the antigen-presenting function of DCs (Donaghy et al., 2001; Kawamura et al., 2003; Lore et al., 2002; Macatonia et al., 1990; Wu and Kewal-Ramani, 2006). The modulation of DCs by HIV infection is a key aspect in viral pathogenesis. It contributes to viral evasion from immunity because the dysfunction of DC engenders some impairment effects for CTL inducement (Donaghy et al., 2003; McMichael and Rowland-Jones, 2001; Rinaldo, 2008; Smed-Sorensen et al., 2004). Furthermore, progressive loss of the DC number and function during the course of HIV-1 infection are reported in Donaghy et al. (2001, 2003) and Macatonia et al. (1990). These findings suggest that the loss of DC number and function in HIV infection might contribute to development of AIDS.

As described herein, we use a simple mathematical model to reveal how loss of the DC number and function correlate with HIV disease progression. Because the progressive decrease of DC number and function are observed (Donaghy et al., 2001, 2003;

* Corresponding author.
E-mail address: dsiwami@ipc.shizuoka.ac.jp (S. Iwami).

0022-5193/$ - see front matter © 2009 Elsevier Ltd. All rights reserved.
doi:10.1016/j.jtbi.2009.06.023

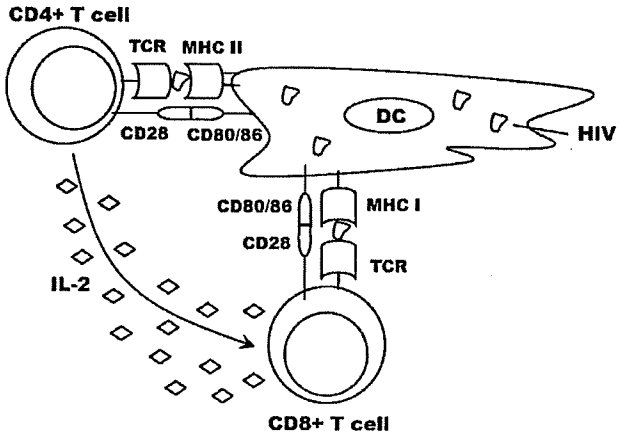

Fig. 1. Summary of function of dendritic cell and its disturbance by HIV infection: after encountering HIV in the peripheral blood, DCs mature and travel to lymphoid organs. The mature DCs present HIV on MHC class II to prime $CD4^+$ T cells to become activated $CD4^+$ T cells, which can secrete helper signals (e.g. IL-2). Furthermore, the DCs cross-present HIV on MHC class I to prime $CD8^+$ T cells. By receiving an antigen signal from the DCs and a helper signal from activated $CD4^+$ T cells, $CD8^+$ T cells expand and differentiate into CTLs to kill HIV infected cells. On the other hand, some DC subtypes are reportedly susceptible to HIV infection. The infection of DCs, for example, reduces expression of the co-stimulatory molecules CD80 and CD86 on the DC surface, which are required for antigen presentation to T cells (to combine with CD28 on the T cell surface). Consequently, the down-regulated expression of CD80 and CD86 engenders subsequent impaired activation of $CD8^+$ T cells.

Macatonia et al., 1990), we simply assumed that the immune impairment effect increases over the HIV infection. Herein, the disease progression dynamics of our model are classifiable into four processes by virological properties. It is particularly interesting a typical disease progression presents a so-called "risky threshold" and an "immunodeficiency threshold" on the impairment rate. Between these thresholds, infected individuals develop to the immunodeficiency phase stochastically depending on their virological and immunological states. Furthermore, to test our theoretical framework, we investigated the existence of these thresholds in 10 patients using previously estimated parameters in Davenport et al. (2004), Mandl et al. (2007), Ogg et al. (1999) and Stafford et al. (2000). We confirmed that all patients take the typical disease progression and that the risky and immunodeficiency thresholds are distributed in similar ranges, irrespective of virological and immunological differences.

Results of our study suggest that a decrease of the immune impairment rate (e.g., we might recover the DC function and increase the DC number by DC immunotherapy, which is a current HIV clinical trial (Connolly et al., 2008; Garcia et al., 2005; Lore et al., 2002; Rinaldo, 2008; Wu and Kewal-Ramani, 2006)) might induce immune responses and delay the disease progression.

2. Materials and methods

For this study, we use a simple mathematical model and previously estimated parameters (Davenport et al., 2004; Mandl et al., 2007; Ogg et al., 1999; Stafford et al., 2000). Here we explain our modeling approach, basic assumptions, and scenario in detail.

2.1. HIV and immune cells dynamics

We describe interactions between HIV and its specific immune responses in the context of immune impairment effects caused by the viral infection. Here, as described in Ciupe et al. (2006) and Stafford et al. (2000), we only consider activated $CD4^+$ T cells (x) as target cells for HIV because other cell populations bearing CD4 molecules such as naive $CD4^+$ T cells, resting $CD4^+$ T cells, and macrophages are less commonly infected by HIV than activated $CD4^+$ T cells are (Ciupe et al., 2006; Hogue et al., 2008; Stafford et al., 2000). We assume that activated $CD4^+$ T cells are produced at a rate of λ cells day^{-1}, decay at a rate d day^{-1} (Ciupe et al., 2006; Stafford et al., 2000), and can become infected at a rate that is proportional to the number of infected $CD4^+$ T cells (y) with a transmission rate constant β day^{-1} $cell^{-1}$ (Iwasa et al., 2005; Wodarz et al., 1998). The infected $CD4^+$ T cells are assumed to decay at the rate of a day^{-1}. To suppress HIV replication, our immune system induces CTL responses through interactions with DCs (see Fig. 1). Here we consider that the CTL responses (z) include both CTL effector and memory (CTL naives are assumed to be described by an initial value of z). The CTL responses eliminate infected $CD4^+$ T cells at a rate that is proportional to the number of CTLs with a killing rate constant p day^{-1} $cell^{-1}$ and decay at a rate of b day^{-1} (Iwasa et al., 2005; Wodarz et al., 1998). We simply assume that proliferation of CTLs (i.e., expansion and differentiation) requires both antigen and a helper signal and that its rate is c day^{-1} $cell^{-2}$. This implies that, in the absence of any immune impairment effects, proliferation is described by $cxyz$ (Altes et al., 2002; Regoes et al., 1998; Wodarz et al., 1998). However, in the presence of immune impairment effects caused by HIV infection, CTL proliferation is reduced (a detailed explanation is provided later). Therefore, we model immune impairment effects as $cxyz/(1+\varepsilon y)$. The impairment effect depends on the number of infected $CD4^+$ T cells; ε represents the immune impairment rate (unit is $cell^{-1}$).

2.2. Mathematical model

We extend the standard virus-immune model including the effect of immune impairment caused by HIV infection (Nowak and May, 2000). Our mathematical model can be represented by the following equations:

$$x' = \lambda - dx - \beta xy,$$

$$y' = \beta xy - ay - pyz,$$

$$z' = \frac{cxyz}{1+\varepsilon y} - bz. \tag{1}$$

Because free virus populations decay at much higher rates than the other T cells, we can assume that the virus population is in a quasi-steady state (Thieme, 2003), and that model (1) (Iwasa et al., 2005; Wodarz et al., 1998) neglects the free virus dynamics.

2.3. Estimation of parameter values

Baseline values of model parameters for simulations and their respective ranges for sensitivity analysis are presented in Table 1. These parameters are based on previously estimated parameters in Davenport et al. (2004), Mandl et al. (2007), Ogg et al. (1999) and Stafford et al. (2000).

Stafford et al. (2000) estimated parameter values of λ, d, β, and a using 10 patients' virus concentration data. They assumed the ratio of activated $CD4^+$ T cells before infection at 1% of the $CD4^+$ T cells in peripheral blood. Here we also use this assumption. Therefore, before infection, we fix the number of activated $CD4^+$ T cells at 10 cells per μl of peripheral blood (i.e., $x_h = 10$ at the healthy state E_h: see Results) because a healthy human adult has about 1000 $CD4^+$ T cells μl^{-1} (Janewa et al., 2004; Nowak and May, 2000). Herein, we can estimate that the proliferation rate of

Table 1
Baseline parameter values for numerical simulations and their ranges for sensitivity analysis: the parameters λ, d, β, and a are set, respectively, to be estimated values based on 10 patients' virus concentration data in Stafford et al. (2000).

Symbol	Description	Value (range)										Reference
		#1	#2	#3	#4	#5	#6	#7	#8	#9	#10	
λ	Proliferation rate of $CD4^+$ T cells ($cells\,day^{-1}$)	0.13	0.2	0.065	0.046	0.17	0.12	0.17	0.085	0.06	0.043	Stafford et al. (2000)
d	Decay rate of $CD4^+$ T cells (day^{-1})	0.013	0.02	0.0065	0.0046	0.017	0.012	0.017	0.0085	0.006	0.0043	Stafford et al. (2000)
β	Infection rate of $CD4^+$ T cells ($cell^{-1}\,day^{-1}$)	0.15027	0.216	0.2048	0.1568	0.1827	0.1975	0.19467	0.1826	0.09167	0.44967	Stafford et al. (2000)
a	Decay rate of infected $CD4^+$ T cells (day^{-1})	0.4	0.8	0.43	0.18	0.39	0.39	0.31	0.17	0.13	0.46	Stafford et al. (2000)
p	Killing rate of infected $CD4^+$ T cells ($cell^{-1}\,day^{-1}$)	0.016										Mandl et al. (2007)
c	Proliferation rate of CTLs ($cell^{-2}\,day^{-1}$)	2.13 (0.426–4.26)										Davenport et al. (2004)
ε	Immune impairment rate of HIV	–										–
b	Decay rate of CTLs (day^{-1})	0.0125 (0.0025–0.025)										Ogg et al. (1999)

We note that β is calculated using original parameter values in Stafford et al. (2000) because we consider that the virus population is in a quasi-steady state. The estimated values of immunological parameters p, c, and b are referred to Stafford et al. (2000), Mandl et al. (2007) and Ogg et al. (1999). We are interested in change of immune impairment effect and their threshold phenomena. Therefore, we need not estimate ε and instead set it as a free parameter.

activated $CD4^+$ T cells is $\lambda = dx_h$ for each patient. Furthermore, we calculate the infection rate of $CD4^+$ T cells β as $\pi k/c$ using original estimated parameter values π, k and c in Stafford et al. (2000) because we neglect the free virus dynamics. Furthermore, we use the estimated values of the decay rate of activated $CD4^+$ T cells d directly, along with those of infected $CD4^+$ T cells a.

Next, we estimate immunological parameter values (which are not based on virus concentration data of the 10 patients). The killing rate of infected $CD4^+$ T cells by CTLs is estimated at $p = 0.016\,cell^{-1}\,day^{-1}$ in Mandl et al. (2007). This parameter does not affect our main results at all (see Results). Therefore, we simply assume that the killing rate is the same in all patients and use it. In Ogg et al. (1999), the mean life-span of CTL effector is estimated as 80 days (i.e., the decay rate is $b = 0.0125\,day^{-1}$). We use the same value for this study. Here, to investigate the sensitivity of the parameter (or a difference among patients), we assume that the CTL decay rate b ranges from $0.0025\,day^{-1}$ (i.e., one-fifth of the value) to $0.025\,day^{-1}$ (i.e., double the value) (because we consider both the CTL effector and memory, we investigate the long-life range of the CTLs). Furthermore, in Davenport et al. (2004), a doubling time of CTLs is estimated as about 18 h. If we assume that $CD4^+$ T cells and infected $CD4^+$ T cells remain at steady state E_u (at which the virus load equilibrates with no immune response: see Results) and the impairment effect is sufficiently small (i.e., $\varepsilon \approx 0$) during a primary expansion and differentiation of CTLs in the acute infection, we can roughly estimate the CTL proliferation rate as $c = 2.13\,cell^{-2}\,day^{-1}$ (we used the average value $x_u = 1.81$ and $y_u = 0.24$ for 10 patients at E_u and the mean decay rate of CTL $b = 0.0125\,day^{-1}$). To investigate a parameter's sensitivity, we assume that the CTL proliferation rate c ranges from $0.426\,cell^{-2}\,day^{-1}$ (i.e., a one-fifth of the value) to $4.26\,cell^{-2}\,day^{-1}$ (i.e., double the value). Moreover, because we are interested in progressive immune impairment effects and their threshold phenomena (see Results), we need not estimate ε and set it as a free parameter.

In Appendix B, we investigate how our mathematical model fits the 10 patients' virus concentration data using our baseline parameter values in Table 1.

2.4. Immune impairment effect over HIV infection

Several DC populations are targets for HIV (Hogue et al., 2008; Lore et al., 2002; Wu and Kewal-Ramani, 2006). Consequently, the ability of DCs (e.g. antigen presentation) to stimulate T cell proliferation is impaired because of the depletion and dysfunction of DC (e.g. downregulation of CD80/86 and MHC II expression) (Donaghy et al., 2001, 2003; Kawamura et al., 2003; Lore et al., 2002; Macatonia et al., 1990; Patterson et al., 1998). The evidence comes from observations that DCs express CD4 and chemokine receptors and are susceptible to HIV infection in vitro (Patterson et al., 1998; Wu and Kewal-Ramani, 2006). Progressive depletion of DC and its functional defects, which would in turn impair generation of CTLs in patients with HIV-1 infection are observed (Donaghy et al., 2001, 2003; Macatonia et al., 1990) and the reduction of DC number and function is particularly marked in patients with AIDS compared with asymptomatic subjects (Macatonia et al., 1990; Patterson et al., 1998). Therefore, the progressive change of DC might contribute to the immunodeficiency associated with HIV-1 disease (Donaghy et al., 2001, 2003; Kawamura et al., 2003; Lore et al., 2002; Macatonia et al., 1990; Patterson et al., 1998; Wu and Kewal-Ramani, 2006). To elucidate how the progressive depletion and functional defect of DCs affect disease symptoms, we simply assume that the immune impairment rate (ε) gradually increases. Therefore, CTL proliferation decreases over the HIV infection. We need not consider dynamics of DC population directly to capture the essence of the progressive immune impairment effect over HIV infection.

3. Results

We investigate how the loss of DC number and function (i.e. increase of immune impairment rate) correlates with HIV disease progression and demonstrate the existence of various thresholds that can determine patients' symptoms.

3.1. Steady states during HIV infection

We explain the virological and immunological meanings of possible steady states of our model (1).

In a healthy human, only activated $CD4^+$ T cells attain an equilibrium level of x_h. We designate this homeostatic equilibrium $E_h = (x_h, 0, 0)$ as a "healthy state" (Nowak and May, 2000).

After infection of HIV, if the basic reproduction number of the virus, $R_0 = \lambda\beta/ad$, is greater than 1, then infected $CD4^+$ T cells increase initially to a high level and subsequently converge to an equilibrium value y_u. Furthermore, activated $CD4^+$ T cells attain an equilibrium level of x_u. This equilibrium $E_u = (x_u, y_u, 0)$ represents a state in which the virus load of HIV is balanced with no immune response because of a shortage of activated $CD4^+$ T cells during a primary phase of HIV infection (Nowak and May, 2000). In this case, we designate the steady state E_u as a "shortage state".

In addition, at the end of the primary phase, if CTL responses are induced, then the infected cells are regulated by them for a long time at some steady state (Janewa et al., 2004; McMichael and Rowland-Jones, 2001). Actually our model has two possible interior equilibria—$E_c^- = (x_c^-, y_c^-, z_c^-)$ and $E_c^+ = (x_c^+, y_c^+, z_c^+)$—but E_c^- is not biologically appropriate because the equilibrium is always unstable even if it exists (see Appendix). Therefore, we consider the equilibrium E_c^+ a "controlled state", in which effective and sustained CTLs have been established and the virus load is suppressed at a low level.

On the other hand, if CTLs are not induced at the end of the primary phase, then the infected individuals immediately develop AIDS after (or during) the acute infection (Binley et al., 2000; Cecilia et al., 1999; Meissnera et al., 2004). Moreover, even if CTLs are induced, the immune responses gradually weaken and some infected individuals, in a late stage of the infection, develop AIDS (Janewa et al., 2004; McMichael and Rowland-Jones, 2001; Tunetsugu-Yokota, 2005). Consequently, when a complete breakdown of the immune system occurs (implying that z converges to 0), activated and infected CD4$^+$ T cells also converge to the same equilibrium values of E_u. In this case, we call the steady state E_u the "immunodeficiency state".

Here we remark that equilibrium E_u has two meanings (the shortage state during the acute infection and the immunodeficiency state over the disease progression) in our model (1). Later in this report, we provide a detailed explanation about the qualitatively different properties of these two states.

3.2. Classification of disease progression dynamics

We assume that the basic reproduction number of HIV, R_0, is greater than 1 and that HIV establishes the infection (Nowak and May, 2000). Herein, we can divide the patterns of disease progression of our model (1) into four cases ((i)–(iv)) (Fig. 2). Because we are interested in the long-term dynamics of HIV

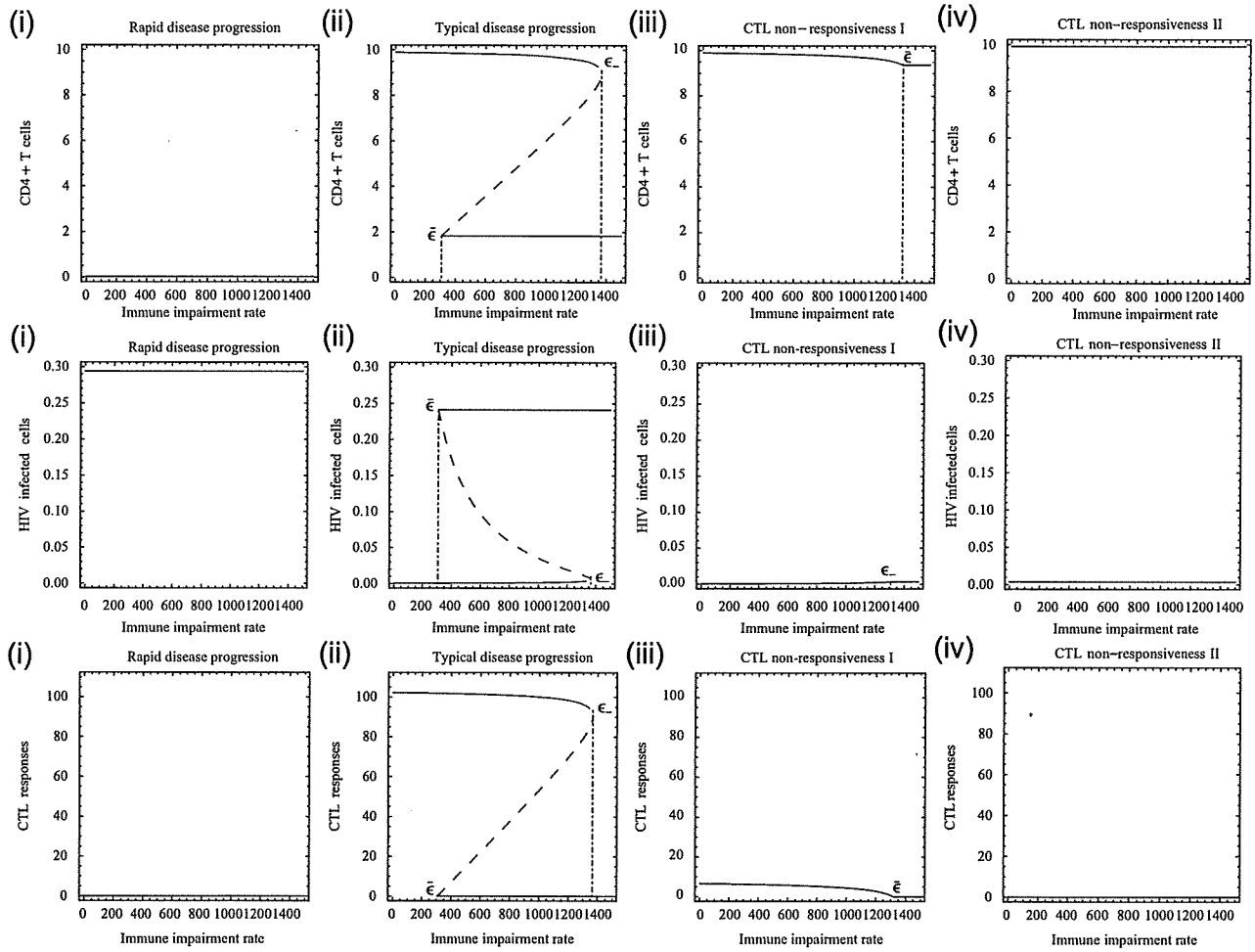

Fig. 2. Classification of disease progression dynamics: the black and red solid lines, respectively, represent each cell number at the controlled and immunodeficiency state over HIV infection (black dashed lines represent each cell number at E_c^-). (i) When the infectivity is large, our immune system does not establish CTL responses in spite of the high virus load because of the depletion of CD4$^+$ T cells. This case corresponds to rapid disease progression of SIV/SHIV infection. On the other hand, when a viral infectivity is small, our immune system can establish sustained CTL responses. Additionally, (ii) if the cytopathogenicity is small (i.e. $0<a<a_-$), then the sustained CTLs suppress HIV replication for a long time. However, the CTL responses decrease gradually and infected individuals come to risk developing AIDS if the impairment rate exceeds the risky threshold (i.e. $\bar{\varepsilon}<\varepsilon$). They always develop AIDS if the rate exceeds the immunodeficiency threshold (i.e. $\varepsilon_-<\varepsilon$). This case corresponds to typical disease progression of HIV infection. Furthermore, regarding (iii) and (iv), if cytopathogenicity is not small (i.e., $a_-<a<\bar{a}$ or $\bar{a}<a<a_{max}$), then CTL responses are slight or nonexistent because of a lack of antigen signals. These cases correspond to CTL non-responsiveness, which differs from immunodeficiency. This phenomenon might be observed in some viral infection with a high degree of cytopathogenicity, but is inapplicable to HIV infection. (For interpretation of the references to color in this figure legend, the reader is referred to the web version of this article.)